Spatiotemporal variability and hydrological characterization of the surface water in the Cuvelai Etosha Basin, Namibia: A flood record

A research thesis submitted in partial fulfilment of the requirements for the honour's degree of Bachelor of Science (Geology)

Of

The University of Namibia

By

Tamekeni Pius Nantuua

200843346

Geology department

12/11/2017

Main supervisor: Dr. Heike Wanke

Co-supervisor: Dr. Martin Hipondoka

Declaration

I, Tamekeni Pius Nantuua, declare hereby that that the research paper titled “the spatiotemporal variability and hydrological characterization of the surface water in the Cuvelai Etosha Basin, Namibia: A flood record, submitted by me is based on actual and original work carried out by me.

No part of this thesis/dissertation may be reproduced, stored in any retrieval system, or transmitted in any form, or by means (e.g. electronic, mechanical, photocopying, recording or otherwise) without the prior permission of the author, or The University of Namibia in that behalf.

I, Tamekeni Pius Nantuua, grant The University of Namibia the right to reproduce this thesis in whole or in part, in any manner or format, which The University of Namibia may deem fit, for any person or institution requiring it for study and research; providing that The University of Namibia shall waive this right if the whole thesis has been or is being published in a manner satisfactory to the University.

…………………………………… ……………………………..........

Tamekeni Pius Nantuua Date

Acknowledgements

First and far most I would like to thank the almighty God for the strength and protection throughout my research work. This wouldn’t have happened if it was not for his merciful allowance.

Secondly I would like to extend my outmost gratitude towards my very supporting supervisor Dr. Heike Wanke. Her patience, motivation, enthusiasm, and immense knowledge in the researched subject has been a strong front towards the success of this work. Conversely I am sincerely thankful for my co-supervisor Dr. Martin Iipondoka for his input and continuous assistance in carrying out meaningful data collection methods. Furthermore I am grateful to Ms Josefina.T. Hamutoko for her exemplary guidance, valuable feedback and constant support throughout the course work of my research. .

A special thank you goes to my family for the inspiration and moral support they have been giving me during the research work. My parents forms the core of my motivation, my spiritual wellbeing and I would far most like to thank them for giving me life, caring for me, and establishing me into the researcher that I am today. Overall I am grateful to my classmate, friends, and to all those that contributed even the slightest addition to this work.

Abstract

Identification and estimation of the physio-chemical evolution of surface water forms an important objective towards characterisation of the basin system as a whole. Baseline information of such a scope can ultimately aid in establishment of vital interlinks of surface water to atmospheric and/or ground water systems. The Cuvelai Etosha Basin (CEB) in northern Namibia is an important water system for both human usage and eco-natural systems. The present study mainly examines the temporal and spatial variation of stable isotope of surface water but a few other complementary physio-chemical parameters are also measured. 224 grab surface water samples were collected during the 2017 CEB wet season over four successive sampling campaigns (February, March, April and May). Sampling cites were randomly selected mainly floodplains (Iishana) and local natural occurring surface water ponds across the Cuvelai drainage region on a minimum sampling spacing of 10km. Physio-chemical parameters turbidity, electrical conductivity and pH were measured for on-site using HACH portable meters. Samples were analysed for stable isotopes (^{2}H and ^{18}O) compositions in the University of Namibia (UNAM) laboratory with an off-axis integrated cavity output spectroscope (Los Gatos Research, DLT-100). Results show pH, turbidity and electrical conductivity varied with time depended on the degree and kind of event captured by the campaigns. Stable isotopes composition range between -13.51 to 12.44 ‰ for δ^{18}O and between -100.08 to 50 .92 ‰ for δ^2H. An evaporation line for the CEB with an equation of $\delta^2H = 5.91\delta^{18}O - 16.7$ is presented by samples collected in March to April. The evaporation line slope is adversely influenced to a higher value by the CEB east surface water. Time series results show a relative decrease in the stable isotope composition in March, coinciding with peak rainfall and flood inflows which concludes to an amount and altitude effect. A progressive increase in the stable isotope composition of the CEB surface water from March to April caused mainly by growing evaporation effect with respect to time is evident. The east and west surface water points to sources with comparatively different isotope compositions. Conclusively, the differences are due to the flood inflow which significantly lowers the composition of the west side of the drainage region to more negative values. There is a lack of significant differences in the isotope composition along the north-south transect which translates to a common storm system affecting the basin. The knowledge spatial and temporal variations of the basin hydrological system will contribute to improved water resource management in the area and provide baseline information to various future scientific studies.

Table of Contents

1. Introduction 1
   1.2 Study area 2
      1.2.1 Physiography 3
      1.2.2 Hydrology and hydrogeological setting 5
   1.2 Problem statement 6
   1.3 Objective of the study 6
   1.4 Hypothesis 7
   1.5 Significance of the project 7
2. Literature review 8
   2.2 Isotopes 9
      2.2.1 Spatial and temporal variations. 13
   2.3 Previous work on the subject 14
      2.3.1 Global scale 14
      2.3.2 Namibia 17
3. Methods and materials 20
   3.1 Sampling 20
   3.2 Analysis 22
4. Results and Interpretation 24
   4.1 Stable isotope 24
   4.2 Physio-chemical parameters 32
5. Conclusion 38
6. Recommendations 40
7. References 41
8. Appedix 45

List of Figures

Figure 1. Location of study area (CEB) in Namibia as circled out by an ellipse object. 2

Figure 2. Geographical and meteorological data for Namibia. (a) Namibia's administrative regions, (b) digital elevation model (DEM), (c) mean annual rainfall, (d) mean annual relative humidity (RH%), (e) mean annual potential evapotranspiration (PET) and (f) mean annual temperature. Source: (Kaseke et al., 2016). 4

Figure 3. The Cuvelai DEM map showing the Cuvelai drainage network. Source: (Mendelsohn & Weber., 2011) 5

Figure 4. (a) Non –equilibrium and equilibrium fractionation effect by progressive depletion and enrichment through a rain out effect. (b) Effect of evaporation on the isotopic composition of surface water and vapour. Source: Mook (2000). 11

Figure 5. Contour plots of $\delta^{18}O$ in Boston Lake water to show the spatial distribution of $\delta^{18}O$ across the Boston Lake influencing area. Source: (Zhou et al., 2016) 15

Figure 6. Dual stable isotope plots of different water systems from North-western China as relative to GMWL and LMWL. Source: (Zhou et al., 2016) 16

Figure 7. Rainfall cokriging isoscapes and the globally fitted isoscape (GFI) overlain with observed data. (a) $\delta^{18}O$ cokriging isoscape, (b) $\delta^{18}O$ GFI, (c) $\delta^{2}H$ cokriging isoscape, (d) $\delta^{2}H$ GFI, (e) d-excess (d) cokriging isoscape, and (f) d-excess (d) GFI (e) d-excess (d) cokriging isoscape, and (f) d-excess (d) GFI (e) d-excess (d) cokriging isoscape, and (f) d-excess (d) GFI. Source: (Kaseke et al., 2016). 17

Figure 8. Modelled local meteoric water lines (LMWL) compared to observation-based LMWL with the global meteoric water line (GMWL). Source: (Kaseke et al., 2016) 19

Figure 9. 2014 sampling results. $\delta^{2}H$ vs. $\delta^{18}O$ from which the Local Meteoric Water Line (LMWL) for the Cuvelai Etosha Basin (CEB) of precipitation (a) and surface water (b) source: (Masiye, 2014). 19

Figure 10. Cuvelai map showing sampling points colour coded to represent different sampling points 21

Figure 11. Sample collecting from (a) local pond (b) A large Oshana (flood plain) 21

Figure 12. Field based measurement set up using HACH portable 22

Figure 13. Sample preparation for the LAP Auto-sampler 23

Figure 14. left, PAL Auto sampler (white) and an off-axis integrated cavity output Laser 23

Figure 15. Box whisker plots showing the variation of the $\delta^{18}O$ and $\delta^{2}H$ over the four sampling campaign respectively. 25

Figure 16. A dual isotope plot of $\delta^{18}O$ vs $\delta^{2}H$ showing the evolution of the CEB surface water through time over four months (February, March, April, and May.____25
Figure 17. Spatial and temporal trends (comparison between Angola and Namibia water on time series).____28
Figure 18. Spatial trend (comparison between the east and west part of the CEB).____28
Figure 19. Temporal trends (May 2014 vs 2017) for the CEB. ____30
Figure 20. Regional comparison of Surface water in southern Africa. ____31
Figure 21. Measured pH and electrical conductivity results. ____33
Figure 22. Electrical conductivity versus chloride content from various sampling campaign collected in 2017. ____34
Figure 23. Electrical conductivity, δ18O [‰] variation with time. From various sampling campaign collected in 2017. ____35
Figure 24. Mean turbidity calculated on month time series from February to April.____36
Figure 25. Frequency pie chart for turbidity result per sampling campaign. ____37

1. Introduction

Water scarcity is a global subject and becomes even further critical for arid and semi-arid countries like Namibia. Sustainable management of this lacking resource requires adequate scientific knowledge of all its sources including surface water (Turewicz, 2012; West et al., 2011). New data is particularly needed in regions currently with poor GNIP coverage, such as in southern Africa (www.iaea.org/water). It is consensus that natural factors like rainfall, surface runoff and groundwater levels are seasonal phenomenon which mainly influence a basin hydrology and are in turn affected by climate (Singh et al., 2004) as cited in (Hajigholizadeh & Melesse., 2016). Natural processes thus by differential magnitude affects the hydrological budget and thereon causing variations in hydrology operatives in space and time. The Cuvelai Etosha Basin (CEB) in central northern Namibia is the main and an important water system for both human usage and eco-natural systems for the local communities. The input budget for the basin are mainly local precipitations and occasional flooding from perennial Angolan counterpart systems. Namibia inconsistent climatic patters shapes its seasonal variations leading to occasional drought and/or flooding which may result in differential effects on the basin isotopic budget. Stable isotopes in water (δ^2H and δ^{18}O) are important indicators of hydrological, ecological pattern and processes (Kaseke et al., 2016; West et al., 2013). Like oxygen isotopes, hydrogen isotopes are conservative tracers of water transport (Yi et al., 2012). This research will nub on the isotopic characterisation (δ^{18}O and δ^2H) of the CEB surface and emphasis will be on the isotopic evolution of the CEB surface water. Results from this campaign will establish means to keep tab and track of CEB water isotope composition through space and time. Similar studies of characterising surface water system have demonstrated substantial contribution to hydrological and hydrogeological solutions all over the globe (Andreo et al., 2004; Bershaw et al., 2012; Honghua et al., 2016; Katsuyama., 2014; Kendall and Coplen., 2001; Ogrinc et al., 2008; Putthividhya & koonthanakulvong, 2011; West et al., 2011;West et al., 2013; Zhou et al., 2016;). The relevance of carrying out such isotopic baseline studies is largely appreciated in multi-disciplinary applied science pertaining to water resource management and monitoring climate-change impacts on local habitants (Turewicz, 2012; Ogrinc et al., 2008). This study exclusively address various hydrological processes effect on the isotopic composition of the basin surface water throughout its course before collecting to atmospheric and/or ground systems. Its findings can contribute towards sustainable management schemes of natural water resources of the CEB and various scientific studies (Araguás-Araguás et al., 1998; Joswiak et al., 2010; Tian et al., 2001; Vuille et al., 2005) as cited in (Bershaw et al., 2012).

1.2 Study area

The study was concentrated in the upper part of the CEB. This area is known to note adverse influences from the Angolan flash floods as marked by an ellipse object (Figure 1). Mainly this is in the Iishana and Nipele sub basin. Few samples however were considered from the far south located sub basins (Olushandja & Tsumeb sub basin) and in the proximal areas of the Angolan counterpart to the CEB. The CEB is the Namibian part of the Cuvelai catchment with ephemeral tributaries systems. The tributaries (locally known as Iishana) only flow during rainy season (Christelis & Struckmeier, 2001).

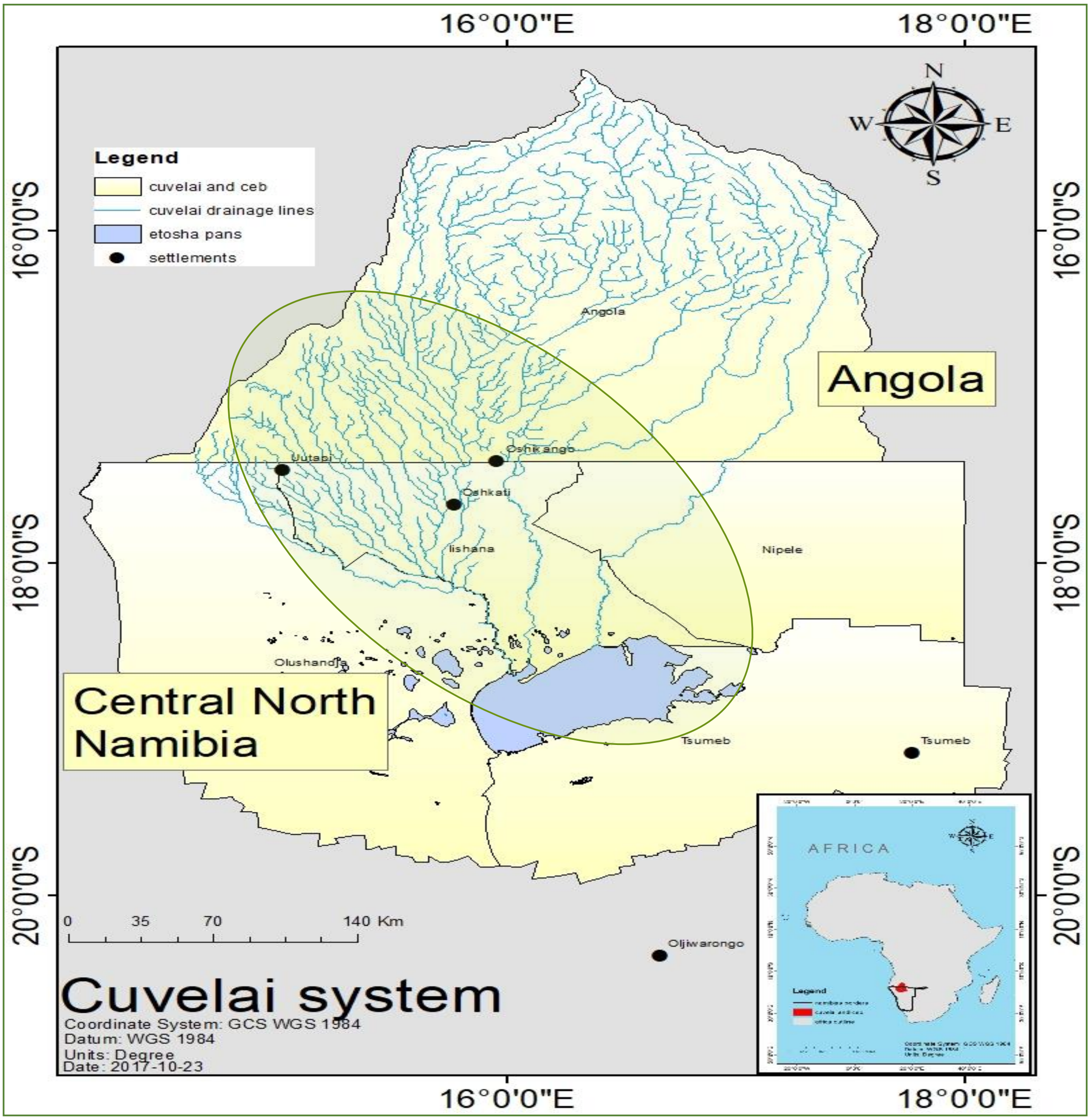

Figure 1. Location of study area (CEB) in Namibia as circled out by an ellipse object.

1.2.1 Physiography

The study area (CEB) is a relatively flat terrain that extends from within Angola towards the southern boundary near Oshivelo (Namibia). CEB is subdivided into four major sub-basins called Iishana, Niipele, Olushandja and Tsumeb (Figure 1). It is a vast sedimentary basin extending covering up to 165,000 km^2 (Hamutoko et al., 2017). The topographic gradient is extremely low, with elevation ranging between 1092 and 1110 metres above sea level (Christelis & Struckmeier, 2001). The drainage is dominantly directed towards the saline Etosha Pan, which is the lowest point in the basin. The area records varying average rainfall ranging, from only 250 mm in the south-western area and west of Ruacana to up to 600 mm in the area around Tsumeb, towards the Kavango Region in the north-east (Bittner, 2006). The eastern portion of the Cuvelai-Etosha has much more consistent rainfalls, than the western section (Mendelsohn et al., 2000) as cited in Dragnich et al, 2004). Almost all rain falls in the summer months between October and March, with the highest falls in December, January and February (Mendelsohn et al., 2013). The Author further stated that the rainfall variability is in the range of 25 % - 40 % and it usually falls during convective thunderstorms. This factor has a direct impact on the presence of surface water and on the groundwater recharge pattern (Ploethner et al., 1997) as cited in (Buttner, 2006). In general high average temperatures combined with an average of three hundred sunny days each year causes potential evaporation to exceed rainfall in Namibia (Dragnich et al., 2004). The CEB climate is characterized as semi-arid with low annual rainfall and high annual temperatures which results in high evaporation rates up to 2000 mm/a (Bittner., 2006) as cited in (Hamutoko et al., 2016). The high annual temperatures, the low humidity, the frequently blowing wind and the limited vegetation cover have much influence on the mean annual potential evapotranspiration which reaches values of about 2,500 mm from September to January as further stated by (Bittner, 2006). On a regional scale the CEB falls within the wettest yet driest part of the country depended on the time of the year. Figure 2 records different meteorological parameters on a larger national scale coverage. These parameters included elevation, mean annual precipitation, mean annual temperature, minimum temperature, mean annual potential evapotranspiration (PET), Aridity Index (AI), and mean annual relative humidity (RH). Data from each of these raster datasets was extracted for each of the 45 data points and we also calculated the straight-line distance from each data point to the Atlantic Ocean (Kaseke., et al., 2016).

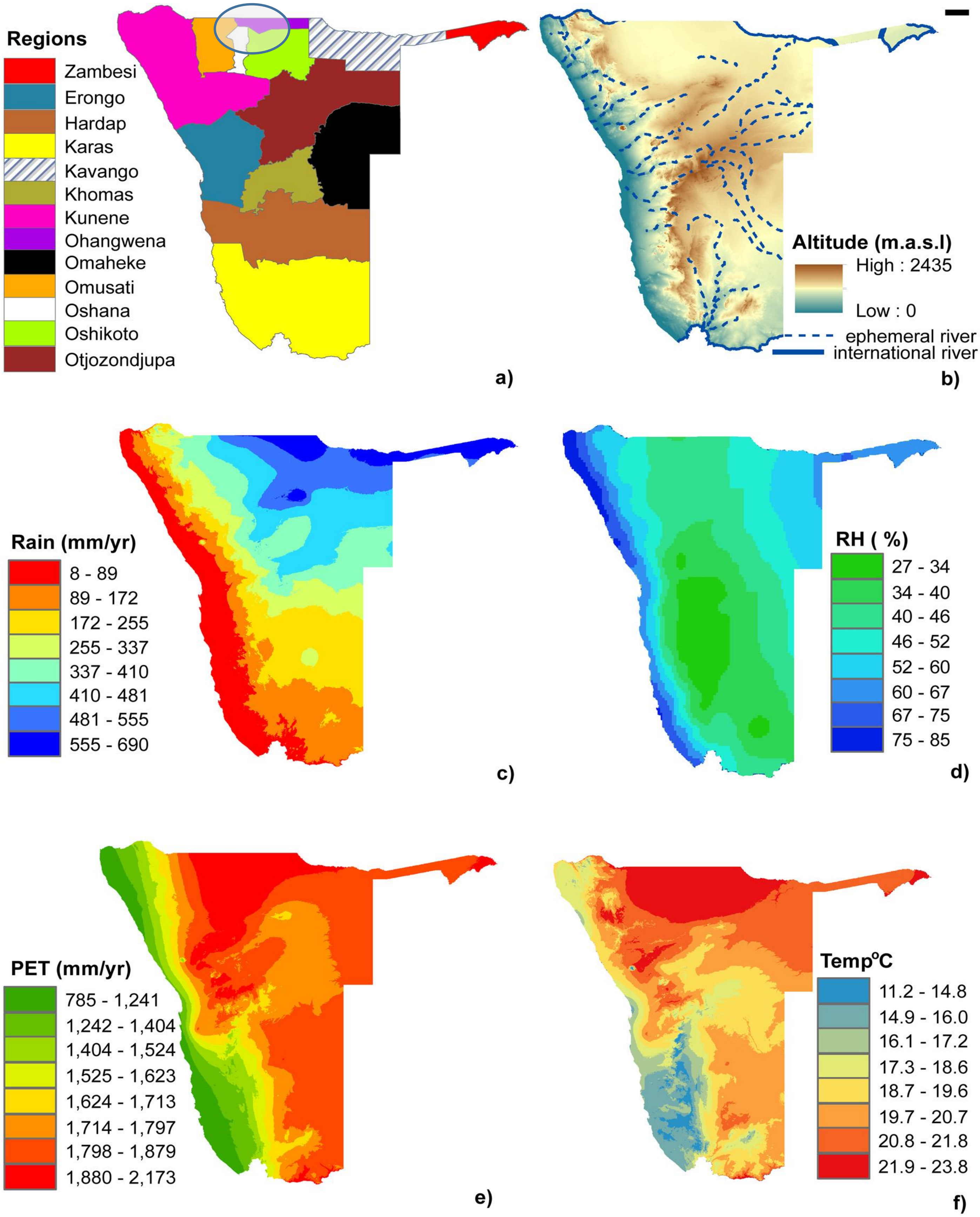

Figure 2. Geographical and meteorological data for Namibia. (a) Namibia's administrative regions, (b) digital elevation model (DEM), (c) mean annual rainfall, (d) mean annual relative humidity (RH%), (e) mean annual potential evapotranspiration (PET) and (f) mean annual temperature. Source: (Kaseke et al., 2016).

1.2.2 Hydrology and hydrogeological setting

The Cuvelai lies within a relatively small depression along the western margins of the vast Kalahari Basin that covers much of south-central Africa (Mendelsohn & Weber., 2011). The topography has a major influence on the entire drainage system. It establishes a scheme of numerous interconnected channels of the Oshana system, cutting into the underlying plane Kalahari sands forming raised, vegetated areas in between Water (Bittner., 2006). The CEB flow schemes feeds from local precipitation and from the upper catchment of the Cuvelai drainage system where recharge occurs at highlands in Angola. The catchment continues into Namibia as a system of interconnected river channels largely shaping the area with ephemeral systems. All rivers in Namibia’s interior including those belonging to the CEB are ephemeral” (Namibia Water Resources Management Review (NWRMR., 2003) as cited in (Dragnich et al., 2004).

Occasionally the flood plains may occur after heavy rainfall and/or floods from Angola (Figure 3). The central north area is drained by a system of Iishinas in varying sizes that leads water to the Etosha Pan via the Oshigambo, Odila and Nipele rivers (Mendelsohn & Weber., 2011). The Cuvelai system consists of two parts, the western part (larger of the two) and the eastern part. The western is more active and is fed primarily by the flooding of rivers flowing off the southwestern foothills of the central Angolan highlands but also by local rains within the system (Stengel., 1963) as cited in (Miller., 2010). He further document that the western part does not receive any water from Angola and is a paleo system fed only by local rains.

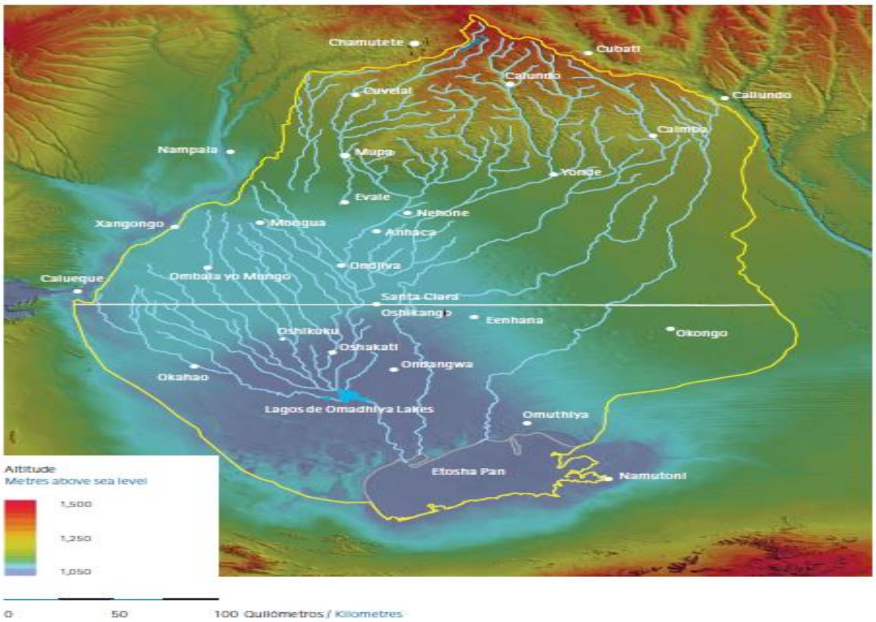

Figure 3. The Cuvelai DEM map showing the Cuvelai drainage network. Source: (Mendelsohn & Weber., 2011)

1.2 Problem statement

Commonly, management in the water resource industry around the globe is hampered by a lack of comprehensive baseline data on specific local hydrological and hydrogeological systems (Honghua et al., 2016; Kaseke et al., 2016; Kendall & Copler., 2001). Previous studies in the Cuvelai Etosha Basin (CEB) have concentrated on the groundwater characterisation and solely on the quality of the surface water for management purposes. The only study of its kind (Masiye, 2014) in the area describes the isotopic composition of CEB water captured from one sampling campaign solely. The study does not further discuss the environmental controls to explain the distribution of the isotopic composition in time and space.

The importance of characterising surface water in physiochemical parameters such as the stable isotopic compositions has been undermined. Thus no record exists that characterises surface water and document ^{18}O and ^{2}H spatio-temporal variability and evolution of the CEB surface water. The characterisation of the surface water is not comprehended and this hampers on scientific capacity for a semi-arid country like Namibia. This shortcoming reflects in the lacking of specific precipitation-surface-groundwater linkage models for the CEB.

1.3 Objective of the study

This study is aimed at assessing the surface water of the CEB in various parameters, with an ultimate focusing goal of understanding the spatial and temporal distribution of the stable isotope (^{18}O and ^{2}H) in surface water in the CEB. Specific objectives of the study are.

- Document temporal and spatial variations of stable isotope of surface water in CEB.
- Determine the environmental factor(s) responsible for temporal and spatial changes (if any is present) on the stable isotopic composition.
- Compare surface water isotopic data from the CEB to existing regional data.
- Identify and characterise differential input sources to the basin surface water system and highlight their origin.

1.4 Hypothesis

The water molecule, whether in rain or river water, carries isotopic ‘fingerprints’ which can be used to determine its origin and transport in the water cycle (www.iaea.org/water/GNIPprogramme). The CEB surface water system is envisaged to be feed directly by precipitation mainly and is known for sporadic occasional overland flows. Sequential subjection thereon to differential isotope composition influencing processes should yield spatial and temporal variations within the system. The hypothesis is based on expectations from mixing dynamic systems and environmental controls voting for so called isotope effects to yield spatial and temporal mappable trends. These trends are envisaged to be mainly functions of latitude, continental and amount effects for the CEB surface water.

1.5 Significance of the project

Documentation of the isotopic composition and other related essential physio-parameters for the surface water in the CEB does not currently exist and yet surface water is a major source and a very influential component to other hydro systems. There is a strong need for additional, continuing, long-term isotope monitoring stations in order to meet current and future scientific data needs (GNIP programme). Characterising the stable isotope distribution in surface waters and estimating their variation within the basin will enable the identification of key parameters essential in the elucidation of the CEB water systems interactions. Such is as an understanding of the exchange dynamics and linkages between CEB’s Surface water, precipitation and ground water. This is e.g. necessary for assessment of the significance of indirect groundwater recharge. Findings from such a study is a fundamental hydrology and hydrogeology objective for a basin or catchment on which possible water resource management, ecological and forensic applications can be based. Specifically the application of the CEB surface water stable isotope data can be utilised in the following studies as adopted from (Yurtsever & Araguas-Araguas, 1993).

- Dynamics of catchment basins (rainfall-runoff processes) (Honghua et al., 2016).
- Distribution of travel times of water in the catchments, or within a surface water body.
- Surface water and groundwater hydraulic interrelations.
- Catchment soil erosion and reservoir siltation rates.
- Mass-transport characteristics of surface waters.
- Isotopes of oxygen, hydrogen, carbon and nitrogen are used to trace the source of pollutants (GNIP programme.)
- Paleo hydrological and Global warming studies in climatology.

2. Literature review

Southern Africa is a globally important meeting point for ocean and climate systems, biological diversity and human societies, yet there is little information on the spatial variability of δ^2H and $\delta^{18}O$ in water across this important region (West et al., 2013). On a globssal scale water is documented as a scarce and yet a very important resource. This account is however even further critical to drier country such as Namibia (Hamutoko et al., 2016; Wanke., 2014; Dragnich et al., 2004). Namibia is the driest country in sub-Saharan Africa (Du Toit & Sguazzin., 1995). The central northern part of Namibia surface water systems by a dominant scale is defined by flood plains locally known as the iishanas. The flood plains collectively shape and facilitate the surface water systems of the basin, nationally known as the CEB. The two recharge regimes to the basin surface water system is direct precipitation and the occasional Cuvelai River flooding from Angola (Dragnich et al., 2004). The basin surface water is subjected to severe evaporation shortly after the offsetting of the rain season. Progressively water quantities are then minimised if not totally lost both to natural and anthropogenic systems eventually. (Mays., 2011) identifies the global hydrological cycle as a system containing three subsystems, the atmospheric water system, the surface water system and the sub-surface water system that are connected in a rather complex structure comprising of various processes. The author further stresses that hydrologic processes transforms the space and time distribution of water in a hydrologic systems throughout the hydrological cycle, in natural and man-made hydraulic systems. The relations of space to time pertaining to hydrologic operatives and their variabilities is an area needs attentive scientific investigation effort. Findings from such studies could create profound milestones solution findings to water management problems. An example of such a study (Mario et al., 2015) realised from the research results that in order to investigate spatially distribution trends and even temporal, one needs to appreciate possible predictor variables and analyse for possible links before analysis for relations are established. In an era of rapid global climatic change, we need spatially explicit and process-oriented baseline information in order to monitor changes to our water resources (West et al., 2011). Changes of the hydrological responses to climate are driven by temperature and precipitation patterns that will affect the temporal and spatial distributions of river source water over time (Marshall & Randhir, 2008). (Zhou et al., 2016) stresses that isotopic compositions of reservoirs will rely on the hydrological balance between inputs (groundwater, precipitation, surface and stream inflows) and outputs (groundwater loss, evaporation, surface and stream outflows). A spatially and temporal explicit map of the stable isotope ratios in water provides an important tool for local scientific studies and ultimately vital contributions to global scientific communities. Global scale studies on stable isotope include such as comparisons between stable isotopes of modern and paleo-waters ($\delta^{18}O$ and δ^2H) to constrain temporal changes in surface elevation and climate [Garzione et al., 2000b; Garzione et al., 2006; Mulch et al., 2010; Poage and Chamberlain, 2001; Quade et al., 2007; Rowley et al., 2001; Saylor et al., 2009;) as cited in (Bershaw., 2012). Precipitation across terrestrial Southern Africa originates as vapour from the Indian and Atlantic Oceans (Van Wyk et al., 2011) as cited in (Kaseke., et al).

2.2 Isotopes

The major parameter for the scope of this study is the stable isotope composition ($\delta^{18}O$ and $\delta^{2}H$) of the surface water. These natural tracers have a large potential for the identification and characterization of different water bodies in hydrological systems, e.g. hydrograph separation, identification of paleo waters vs. present-day groundwater, mixing processes between groundwater and surface waters (Froehli et al., 2000). Stable isotopes are good recorders of ecological pattern and process (West et al., 2006) and of many more important temporal and spatial variations. This variations are reflective of influences from topography, climate, water migrations and groundwater evolutions. Isotope fractionation forms the underlying phenomenon for isotope studies and is widely recorded by literature as the basis for isotope differential abundances and variation in the hydrosphere (Turewicz, 2012). (Clark & Frits, 1997) argued that thermodynamic fractionation is a fundamental process. Such a partition is due to differential rates of reaction for different molecular species. The author further describes the partition to result as disproportionate concentration of one isotope over the other on one side of the reaction. (Mook., 2000) links the portioning to at least three processes namely physicochemical fractionation, diffusive fractionation isotopic equilibrium and kinetic (non-equilibrium) fractionation. Kinetic fractionation is from irreversible processes such as the evaporation of water with immediate withdrawal of the vapour from further contact with the water whilst the latter is involved in a (thermodynamic) equilibrium reaction. Heavier isotopes ($^{1}H_2{}^{18}O$ and $^{1}H^{2}H^{16}O$) have lower mobility, higher binding energies, lower vapour pressures than $^{1}H_2{}^{16}O$ and thus evaporate less easily (Mook., 2000). The author further states during physical processes isotopically lighter molecules have higher velocities and smaller binding energies. In chemical processes light molecules are more than the heavy molecules. In some cases, however, the opposite is true. This inverse kinetic isotope effect occurs most commonly in reactions involving hydrogen atoms (Bigeleisen and Wolfsberg, 1958) evaporation largely dictates the initial isotopic evolution of water in the hydrological cycle.

The isotopic composition difference ($\delta^{18}O$ and $\delta^{2}H$) of precipitation and its source vapour has been explained using the Rayleigh distillation mechanism. The effect of Rayleigh distillation effects are summarised in (Bershaw et al., 2012). Rayleigh distillation of an air mass under equilibrium conditions without local evaporation or advection of additional vapour from outside the system causes a progressive decrease in the $\delta^{18}O$ and $\delta^{2}H$ values of precipitation (Craig & Gordon, 1965; Dansgaard, 1964; Friedman et al., 1964; Gat and Dansgaard, 1972; Merlivat & Jouzel, 1979; Rozanski et al., 1993; Siegenthaler & Matter, 1983; Taylor, 1972) as cited in (Rozanski et al., 1993). However, the preceding of sub cloud evaporation of raindrops can apparently significantly attenuate this decrease in $\delta^{18}O$ and $\delta^{2}H$. (Mook, 2000) describes Initial Ocean evaporation isotopic partitioning to be due the difference between the vapour pressure of the overlying air and the saturated vapour pressure at the temperature of the evaporating surface (saturation deficit). Evaporation is known to take its toll once again when water reaches the earth surface, either directly from surface water, the wet soil surface or from interception on the vegetation. The evolution of isotope composition between the precipitation and condensation phases is schematically represented (Figure 4a), adopted from (Mook, 2000). Initial marine water is subjected to non-equilibrium evaporation and the first vapour is formed (clear box 1) resulting in the remaining water to be isotopically depleted, the precipitation derived from this vapour however (box 1) is then isotopically enriched and so is the produced precipitation (black box 1). This progressive depletion and enrichment stepwise evaporation and condensation process generates the so called rainout effect. Isotopic variation is further caused by successive depletion of water, clear box 1 to 3 and consequentially enrichment in vapour from black box 1 to 3 (Figure 4b).

The $\delta^{18}O$ and $\delta^{2}H$ contents of precipitation are then subjected to further continental evaporation and mixing in between precipitations, surface water and ground systems. Isotope fractionation is a thermos dependent reaction, as proved by the existence of a correlation between $\delta^{18}O$ in rainwater and environmental temperature (Dansgaard., 1964: Siegenthaler & Oeschger., 1980) leading to conclusion that the higher the process temperature, the higher the heavy isotope and thus in turn the degree of fractionation increases with temperature.

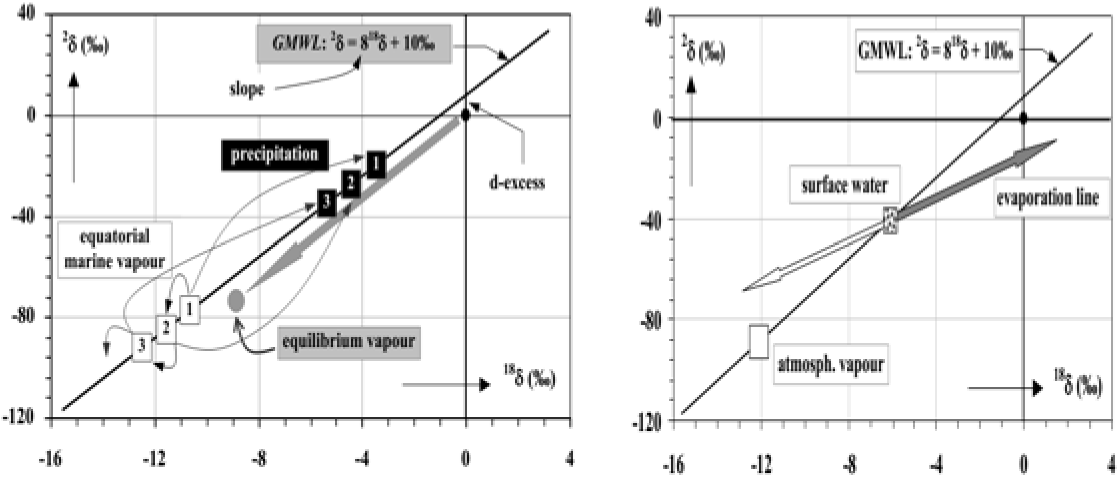

(a) (b)

Figure 4. (a) Non –equilibrium and equilibrium fractionation effect by progressive depletion and enrichment through a rain out effect. (b) Effect of evaporation on the isotopic composition of surface water and vapour. Source: Mook (2000).

The hydrological cycle is a complex entity comprising of various steps, each with its partitioning participation of $\delta^{18}O$ and $\delta^{2}H$. Nonetheless their behaviour is still predictable and this was published in (Craig., 1961) as cited in (Clark & Frits, 1997) as there exist a correlation between $\delta^{18}O$ and $\delta^{2}H$ with linear regression value (correlation coefficient) $r^{2} > 0.95$. As cited in (Masiye, 2014), (Kendall et al., 1995) asserted that a high correlation coefficient reflects the fact that ^{18}O and ^{2}H in water molecules are closely related and this is documented as the Craig's global meteoric water line (GMWL) as indicated in (Figure 4a & 4b) and is represented by equation.

$$\delta^{2}H = 8\ \delta^{18}O + 10‰$$

Local Meteoric water line (LMWL) can however be locally derived to represents precipitation from a single and/or local sites. Slight deviations are expected due to differences in relative humidity and are seen much when water is subjected to evaporation. Important interpretational parameters are realised from such a regression line and this include, slope (s) which is 8 and may locally deviate from that of the GMWL. D-excess (d) is referred to as the deuterium excess is the intercept with the $\delta^{2}H$ axis. A deuterium excess (d excess) in water results from isotope fractionations and is mathematically presented by (Dansgaard, 1964) as a function of deuterium (^{2}H) and heavy oxygen (^{18}O) in water by equation

$$D\ excess = \delta^{2}H - 8\ \delta^{18}O$$

The value is recorded by (Celle-Jeanton et al., 2001; Cruz Sanjulia´n et al., 1992; Rindsberger et al., 1983;) as cited in (Andreo et al., 2004) as an indication of the origin of the water. D-excess if known, can provide information about the climate conditions of the moisture source (Katsuyama et al., 2014). Points that fall on the Global Meteoric Water Line (GMWL) have a constant d of 10‰ because rainout isotopic fractionation is considered an equilibrium process (Kaseke et al., 2016). It is apparent that d values close to 10% indicate waters of Atlantic origin, values close to 22% are characteristic of waters from the Eastern Mediterranean and d values close to 14%, intermediate between the first 2, are detected in rainwater falling on the western Mediterranean. Vapour derived from the Indian or Pacific Oceans clocks about 10‰ (Gat and Carmi., 1970) as cited in (Bershaw., et al 2012). Several authors however have argued against conclusive direct inferring of vapour origin using d-excess value alone. 'd' excess values can also vary significantly based on local environmental conditions, such as the temperature of condensation, amount of sub cloud evaporation during rainout, and degree of local moisture recycling (Jouzel & Merlivat, 1984; Gat & Airey., 2006; Liotta et al., 2006; Froehlich et al., 2000; Kurita & Yamada, 2008; Cui et al., 2009) and (Lai et al., 2011; Welp et al., 2012; Zhao., et al 2014) as cited in (Kaseke et al., 2016) In parallel with this judgement, (Merlivat & Jouzel, 1979) showed that the d-excess in air masses and hence of precipitation depends on the relative humidity of the air masses at their oceanic origin, the ocean surface temperature, and kinetic isotope effects during evaporation.

Generally High d-excess values are seen as an indication that more evaporated moisture has been added to the atmosphere (Gat & Matsui, 1991), and low values are associated with samples fractionated by evaporation. Water subjected to continental evaporation is commonly seen to plot below the GMWL and/or LMWL depended on water residence time, relative humidity and thus degree of evaporation. The mean potential evaporation rate of the CEB can be as high as 3000 mm/a, which is five times higher than the precipitation (Christelis & Struckmeier., 2001) as cited in (Hamutoko et al., 2017). High evaporation factor is thus expected to significantly modify the stable isotopic composition of the water to more ^{18}O enrichment relative to ^{2}H with respect to local meteoric water compositions.

2.2.1 Spatial and temporal variations.

Continental processes that precedes initial evaporation of marine water and thereon condensation shapes the spatial and temporal local isotopic trends. The trends are documents by hydro scientist as catchment isotope effects. Such is as the subsequent alterations of the precipitation compositions by rain out effect, selective recharge, runoff, mixing with older groundwater and newer rain water, and environment controls such evaporation according to (Dansgaard., 1964; Gat & Tzur., 1967) as cited in (Masiye, 2014). (Dansgaard., 1964) says, based on the assessments of early data compiled by the IAEA (International Atomic Energy Agency)/WMO (World Meteorological Organization) network, a number of environmental parameters characterizing the sampling site, such as, the latitude, altitude, distance from the coast, the amount of precipitation and the surface air temperature have an influence on the distribution of the heavy isotopes ^{18}O and ^{2}H in meteoric waters. Moreover (Dansgaard., 1964; Eriksson., 1983; Fritz and Fontes., 1980; Rozanski et al., 1992; Plata, 1994) as cited in (Andreo et al., 2004) postulated the following.

- Atmospheric moisture decreases with an increase in the concentrations of ^{18}O and ^{2}H in the vapour phase).
- Rainfall intensity (amount) increases with a decrease in the heavy isotope content (Matsuo and Friedman, 1967; Miyake et al., 1968; Ambach et al., 1975) as cited in (Rozanski et al., 1993). (Mook, 2000) however argues that this generalisation is not always applicable and thus local amount effect should be individually and in detail locally scrutinised.
- Latitude is inversely proportional to heavy isotope content, thus latitude increases with a decrease in the heavy stable isotope contents
- Altitude is inversely proportional to heavy isotope content, meaning the elevation increases with a decrease in the heavy stable isotope content).
- The continental effect which is in turn a function of higher elevation and distal expanse from the sea votes for a progressive decrease in the heavy isotope content.
- The seasonal effect (summer rainfalls have higher heavy isotope content than winter rainfalls). Winter rainfall is generally more abundant and isotopically depleted (Andreo et al, 2004).

The stable isotopic composition of groundwater (expressed as abundance of oxygen-18 and deuterium) is determined by the isotopic composition of recharge. The isotopic composition of the groundwater will thus mirror much the most contributing recharge if influence by differential input systems. It is important to identify and know the proportions of these recharge components in order to increase the sustainable supply of water to various use and thus supplying eminent baseline information to water management strategies. The interlinks of surface water and groundwater however can be better understood with an integration of several hydro models at least including an isoscape.

2.3 Previous work on the subject

2.3.1 Global scale

A study on characteristics of stable isotopes in an inland Lake and their implications for water management in North-Western China was undertaken in 2016. According to (Zhou et al., 2016). The study reported for samples from Bosten Lake, Kaidu River, groundwater near the lake and one agricultural and industrial wastewater near Bosten Lake using laser absorption water isotope spectrometer analyser (Model DLT-100, Los Gatos Research Inc.). The study aimed at determining the distribution of stable isotopes by studying the spatial-temporal variations of δ^{18}O and performing hydrograph separation on Bosten lake and rivers. A spatial map was produce to show the variation of δ^{18}O across the Boston Lake**.** Four Different components of lake water (river runoff, groundwater, agricultural and industrial drainage, and local precipitation) and their contribution proportions was quantified as 31%, 35%, 25%, and 9% respectively. It is was deliberated that comparing the stable isotope (δ^{18}O and δ^{2}H) of different water samples using the global meteoric water lines (GMWL) and local meteoric water lines (LMWL) was useful. For example it was essential for clarifying the water source and isotopic fractionation for the study of regional hydrological processes. According to (Zhou et al., 2016) it is best to use δ^{18}O to analyse the spatial and temporal variability due to its enhanced stability compared to δ^{2}H.

The δ^{18}O - δ^{2}H correlations are strong and distinguishable among river Basins (Yi et al., 2012). The δ^{18}O ranged from −0.27‰ to −9.99‰ with an average of −3.53‰. A general trend was seen and described as low δ^{18}O diffused from south to west, and high δ^{18}O diffused from north to west. Temporal trends were realised and largely affiliated to seasonal changes. The average δ^{18}O values of the Bosten Lake water were relatively high in summer (from June to August) but low in winter (Zhou et al., 2016). The data records δ^{18}O values of the water samples collected along the Kaidu River ranging from −8.99‰ to 13.33‰ and a mean of −10.14‰. The δD (δ^{2}H) values ranged from −66.02‰ to 90.42‰, with a mean of 72.36‰ (Figure 6a). These values plotted above the GMWL and LMWL and was interpreted to indicate that local runoff water was derived from local ice and precipitated at low temperature. The data was also used to compare groundwater and runoff (River water) and since they had similar isotopic signatures, they are believed to have a common source. The δ^{18}O values of the surface water samples however ranged from −0.28‰ to 9.61‰, with an average of −4.10‰. The δD values ranged from −14.12‰ to −66.25‰, with an average of -29.15‰. as shown by (Figure 6b), stable isotope values of the water from Bosten Lake were increased compared with the water from the Kaidu River and Huangshuigou River runoff (Zhou et al., 2016). The isotopic composition of river water, groundwater, agricultural and industrial wastewater, and precipitation in the Yanqi Basin plotted near the LEL concluding that the four water sources recharged from evaporated water (Boston Lake).

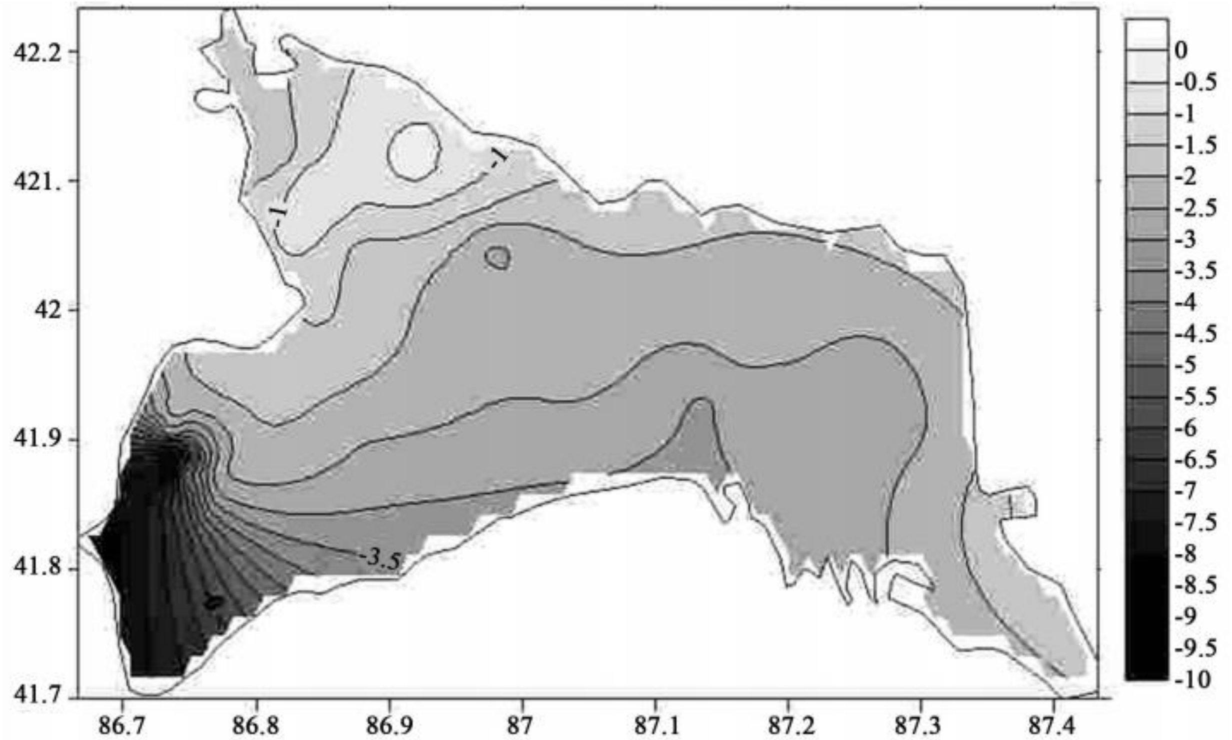

Figure 5. Contour plots of $\delta^{18}O$ in Boston Lake water to show the spatial distribution of $\delta^{18}O$ across the Boston Lake influencing area. Source: (Zhou et al., 2016)

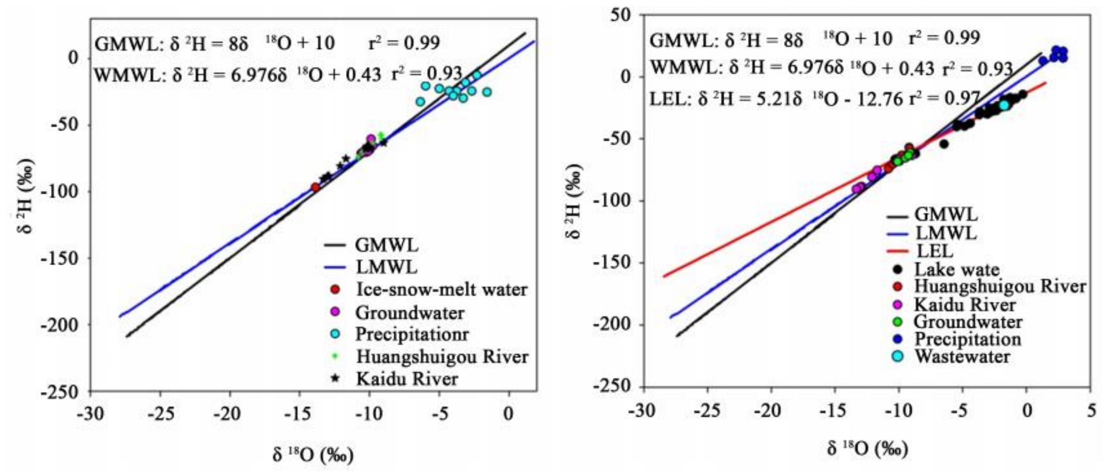

(a) (b)

Figure 6. Dual stable isotope plots of different water systems from North-western China as relative to GMWL and LMWL. Source: (Zhou et al., 2016)

(Carol Kendal & Tyler B. Coplen., 2001) studied the distribution of oxygen-18 and deuterium in river waters across the United States with an aim to remedy the difficulties in reconstruction of continental paleo-climate and paleo-hydrology relative to modern hydrological regimes. The research used more than 4800 stream samples from 391 selected sites within the USGS National Stream Quality Accounting Network (NASQAN) and Hydrologic Benchmark Network (HBN). This data now serves as a proxy for the isotopic composition of modern precipitation in the USA (http://water.usgs.gov/pubs/ofr/ofr00-160/pdf/ofr00-160.pdf). The idea was prompt by the fact that the only isotopic data available was from the only long-term regional network for collection and analysis of precipitation for in the USA (and world) is the Global Network for Isotopes in Precipitation (GNIP) established by a collaboration between the International Atomic Energy Agency (IAEA) and the World Meteorological Organization (WMO). From the isotopic distribution of δ^{18}O and δ^{2}H, the study concluded that slow water circulation and strong evaporation in the lake resulted in the high δ^{18}O. The author further realised irrigation drainage and industrial wastewater, enriched high TDS, were the main factors affecting the water quality of Bosten Lake.

A similar study on spatial and seasonal variations of δ^{18}O and δ^{2}H values in the River Sava in Slovenia using in total 345 river and 41 groundwater samples were collected during the observation period. The results showed that the water originated mainly from Atlantic Ocean but an influence from the Mediterranean ocean was also evident. The mean residence time in the main stream water of the River Sava was estimated to be 1.32 years and is in a good agreement with the residence time determined using ^{3}H measurements (Ogrinc et al., 2008). The authors claim the data extended their knowledge in understanding the hydrological cycle of the River Sava, the interactions between precipitation, surface water and groundwater and, at the same time, demonstrate the utility of isotope tracers in determining catchments characteristics.

2.3.2 Namibia

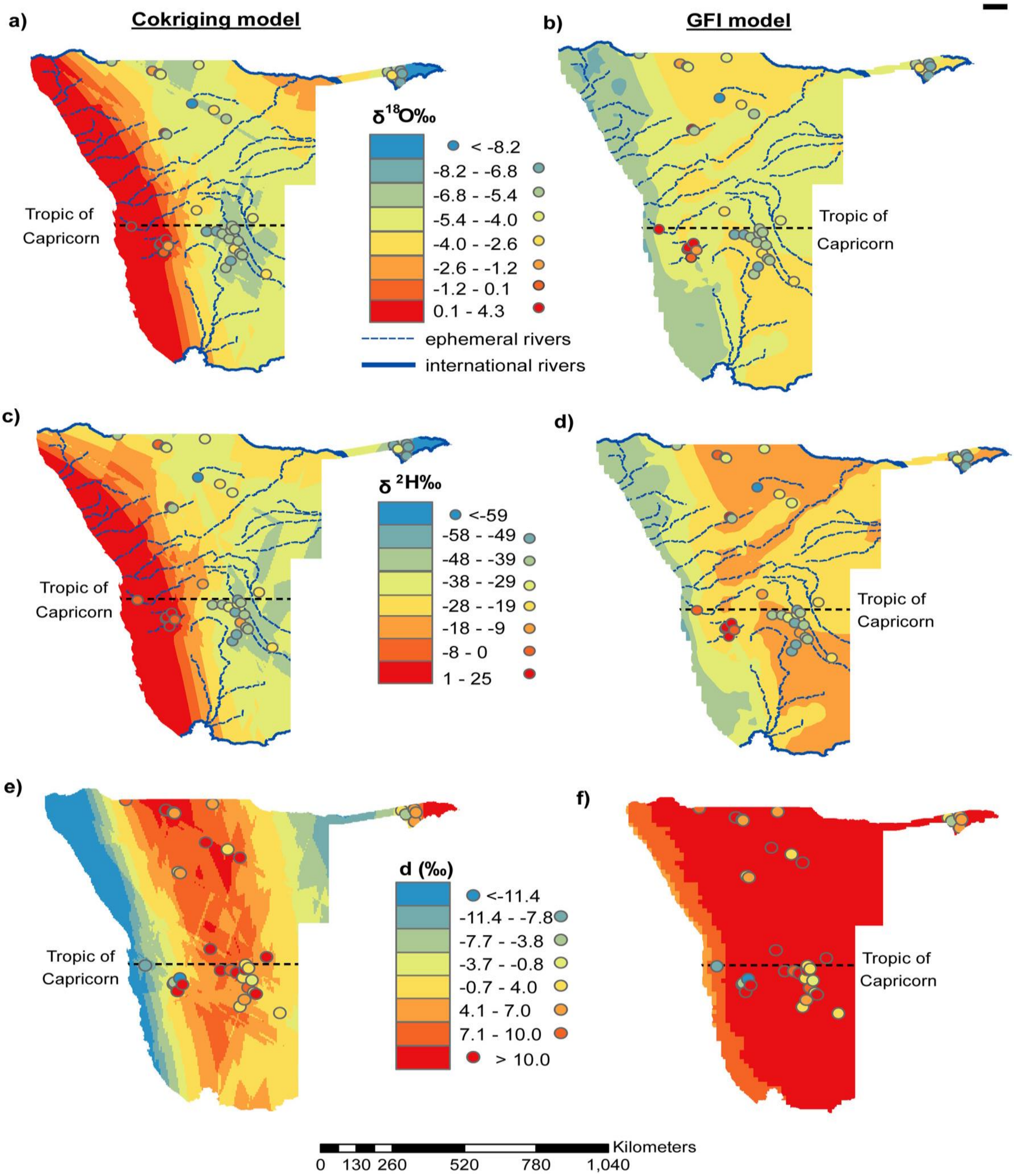

Figure 7. Rainfall cokriging isoscapes and the globally fitted isoscape (GFI) overlain with observed data. (a) $\delta^{18}O$ cokriging isoscape, (b) $\delta^{18}O$ GFI, (c) δ^2H cokriging isoscape, (d) δ^2H GFI, (e) d-excess (d) cokriging isoscape, and (f) d-excess (d) GFI (e) d-excess (d) cokriging isoscape, and (f) d-excess (d) GFI (e) d-excess (d) cokriging isoscape, and (f) d-excess (d) GFI. Source: (Kaseke et al., 2016).

(Kaseke et al., 2016) presented nationwide rainfall isotope date (figure 7) on rainfall using the cokriging method and compared it to a globally fitted isoscape (GFI). Consistently shown for both δ^2H and $\delta^{18}O$ by the cokriging method is the continental effect, pointing to Atlantic Ocean as the source for precipitation. The GFI however supports as the source following depletion trend from the east moving west although the author describes a poor relation ($R^2 = 0.11, p < 0.05$) to support the continental effect from the Indian ocean. (Figure 8) documents LMWL for the CEB developed from different approaches and all points towards a similar slope of ± 7.2. The author however has advised that the modelled Namibian GFI-LMWL reflects the average isotopic composition of global meteoric waters and does not account for local variations even when scaled down to a smaller geographic area.

The CEB LMWL has a slope of 7.2 and an intercept of +4.4 ($\delta^2H = 7.2\ \delta18O + 4.4$; $R^2 = 0.99$) and was developed from rainfall data collected within SASSCAL between 2013 and 2015 and historic data compiled by (Turewicz, 2012). In 2014, a study was undertaken with an aim of understanding the geospatial distribution of ^{18}O and ^2H in precipitation and surface-water in the CEB (Namibia). (Masiye, 2014) produced a plot (Figure 9) $\delta^{18}O$ vs δ^2H and interpreted the results as concurrent with Craig's postulation on $\delta^{18}O$ and δ^2H relations. The figure is a representation of the surface water evaporation which indicates an evaporation line for the (CEB). The evaporation line has a slope of 4.91 and R^2 value of 0.97 as initially defined by (Masiye, 2014). This was however done using data from one sampling campaign and thus may change as isotopic composition varies with time as a consequence of hydrological operatives. Water that has undergone evaporation or mixed with evaporated water generally plots below the GMWL. Surface water typically have slopes in the range 2 to 5, which is consistent with Craig's findings substantiated in (Kendall et al., 1995). (Masiye, 2014) however did not do time series analysis of the surface water isotopic composition to reflect its evolution through time. (Hamutoko et al., 2017) characterised the CEB groundwater, focusing on shallow perched aquifers with respect to deep aquifer by physico-chemical parameters. The study indicated that the deep wells are highly mineralized in comparison to shallow wells using EC discriminatory and recorded values ranging from 489 to 1199 µS/cm and 52 to 296 µS/cm respectively for the deep wells. TDS values were in parallel with the EC in that it attained high values in deep wells relative to shallow wells the author revealed. Shallow wells recorded a pH of about 7.1 and the deep well of about 7.6. The study further considers the geochemistry of shallow groundwater and was linked to the prevailed evaporation, pointing out in parallel to (Obiefuna & Orazulike., 2011) that evaporation increases the concentration of ions in the remaining water and leads to precipitation and deposition of evaporates. The stable isotope analysis resolved that the samples collected from shallow wells follow a regression line of $\delta^2H = 4.66\ \delta^{18}O - 14.65$; R2 = 0.94. Samples from deep wells plot on a regression line with an equation of $\delta^2H = 6.01\delta^{18}O + 7.88$; R2 = 0.93 (Hamutoko et al., 2017). The author further indicated that the isotopic composition of oxygen and hydrogen in shallow well water ranges from −6.95 to 0.86‰ and −49.1 to −7.6‰ for $\delta^{18}O$ and δ^2H, respectively. For deep wells, $\delta^{18}O$ values vary between −9.00 and −1.30‰ and for δ^2H between −61.5 and −22.1‰).

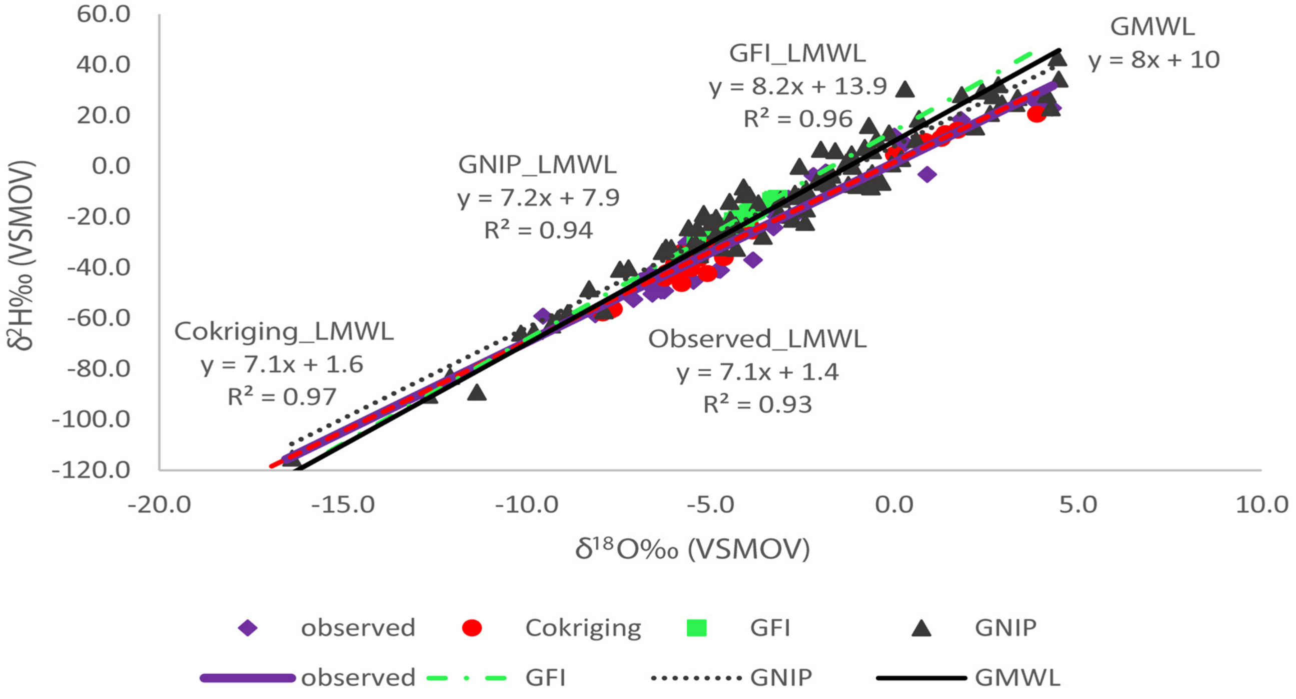

Figure 8. Modelled local meteoric water lines (LMWL) compared to observation-based LMWL with the global meteoric water line (GMWL). Source: (Kaseke et al., 2016)

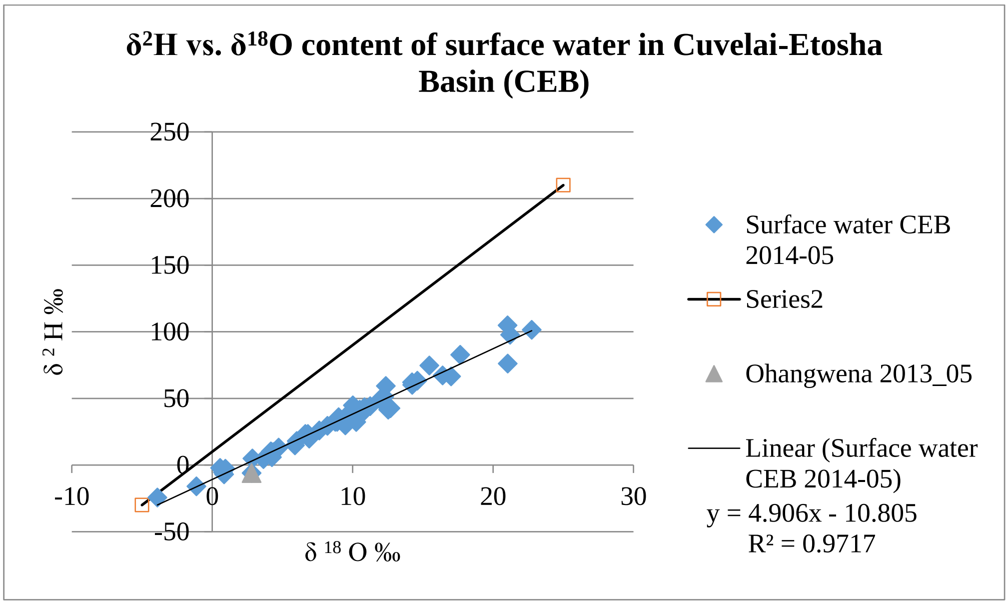

Figure 9. 2014 sampling results, δ^2H vs. $\delta^{18}O$ presenting Local Meteoric Water Line (LMWL) for the Cuvelai Etosha Basin (precipitation) and evaporation line (surface water) Source: (Masiye, 2014).

3. Methods and materials

The present research integrated quantitative analysis and qualitative interpretation of identified trends. Methodologies used comprises of a program that involved Desktop studies, sample collection and/or acquiring of pre-existing data, data processing and interpretation in a sequentially order over a period of 10 months during the year 2017. The desktop study involved integrating various type of data of interest to research. Mainly this was such as available local isotope data, area hydrology descriptive information, and similar studies up to national scale. This was essential to understanding the rainfall, climate and flooding existing records in order account for hydrological events with isotope content altering potentials. Following the identification of critical peaks of hydrological events, a plan was then accordingly designed to capture the events using a systematic sampling campaign. The sampling was done over the wet season of the CEB system and concentrated along the Cuvelai drainage networks as shown by the map (Figure 10). Dual isotope scatter plot analysis were then used to study the variations and evolution of the CEB surface water. Stable isotope hydrology is based on interpreting isotope variations (δ^2H, δ^{18}O and d-excess) which are governed by the origins and conditions during cloud formation and rainout (Stumpp et al., 2014) as cited in (Kaseke et al., 2016).

3.1 Sampling

The sampling was done during early months of the wet season 2017, samples were obtained over a four sampling campaign with each having a sampling periodicity of one week. A Total of 224 Grab surface water samples (50ml) were collected from flood plains (Iishana) and local surface ponds. The sampled catchments were of varying sizes on a minimum 10km sampling spacing density as shown in figure 10. The four sampling times were selected to capture main hydrological events that affected the CEB surface water system. Campaigns ranged from the initial surface water accumulation after first precipitations, through occasional flash flooding events and finally after sometime of evaporation dormant exposure. This sequence of events were systematically measured for on monthly series, specifically February, March, April and May. Water samples were collected from different surface water sites within the borders of Namibia as well as at several sites within the borders of Angola as shown by figure 10. The samples were collected in 50 ml borosilicate glass and several polyethylene bottles (HDPE), air tightly closed and shipped to the University of Namibia for laboratory analysis. The sampling involved tapping water from natural catchment features such as natural ponds, flood plains, rivers and any other surficial depression that held surface water. Avoidance was for deeper depression and surface water accumulation with proximal or direct influence from groundwater systems. All the samples were similarly measured for complementary characterising parameters on site such as temperature, pH, electrical conductivity and turbidity.

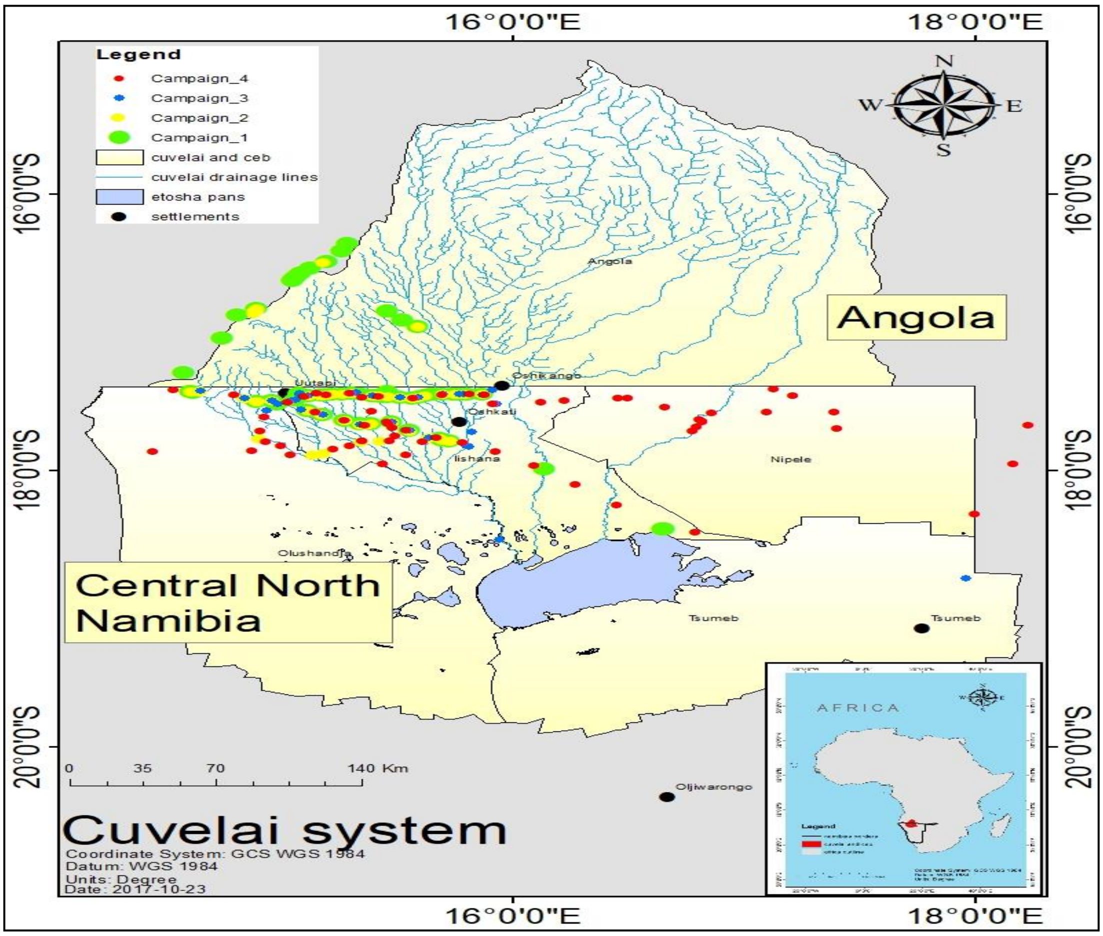

Figure 10. Cuvelai map showing sampling points colour coded to represent different sampling points

Figure 11. Sample collecting from (a) local pond (b) A large Oshana (flood plain)


[redacted]

Figure 12. Field based measurement set up using HACH portable

3.2 Analysis

Complementary parameters such Electrical conductivity, pH, and turbidity were all measured for on-site using HACH portable meters as shown in figure 12. All samples chloride content was analyzed at University of Namibia (UNAM) using a HACH chloride meter. Similarly $\delta^{18}O$ and $\delta^{2}H$ were measured using an off-axis integrated cavity output spectroscope (OA-ICOS, Los Gatos DLT-100) in collaboration work with an LAP auto sampler as shown in figure 13 and figure 14 respectively. Isotope concentrations are expressed as rations of the sample with respect to a standard sample as it deviates from 1 according to equations.

$$\delta^{18}O_{\mathrm{SAMPLE}} = \left\{ \frac{\left({}^{18}O/{}^{16}O\right)_{\mathrm{SAMPLE}}}{\left({}^{18}O/{}^{16}O\right)_{\mathrm{VSMOW}}} - 1 \right\} \times 10^{3}$$

$$\delta H_{\mathrm{SAMPLE}} = \left\{ \frac{\left({}^{2}H/{}^{1}H\right)_{\mathrm{SAMPLE}}}{\left({}^{2}H/{}^{1}H\right)_{\mathrm{VSMOW}}} - 1 \right\} \times 10^{3}$$

Three other standards (very depleted, very enriched and snow isotopic composition) were used along with (VSMOW). The isotope compositions are reported using notation (δ). $\delta^{18}O$ and $\delta^{2}H$ were measured with average standard deviation (sd) of 0.12 and 0.69 for $\delta^{18}O$ and $\delta^{2}H$ respectively.

Figure 13. Sample preparation for the LAP Auto-sampler

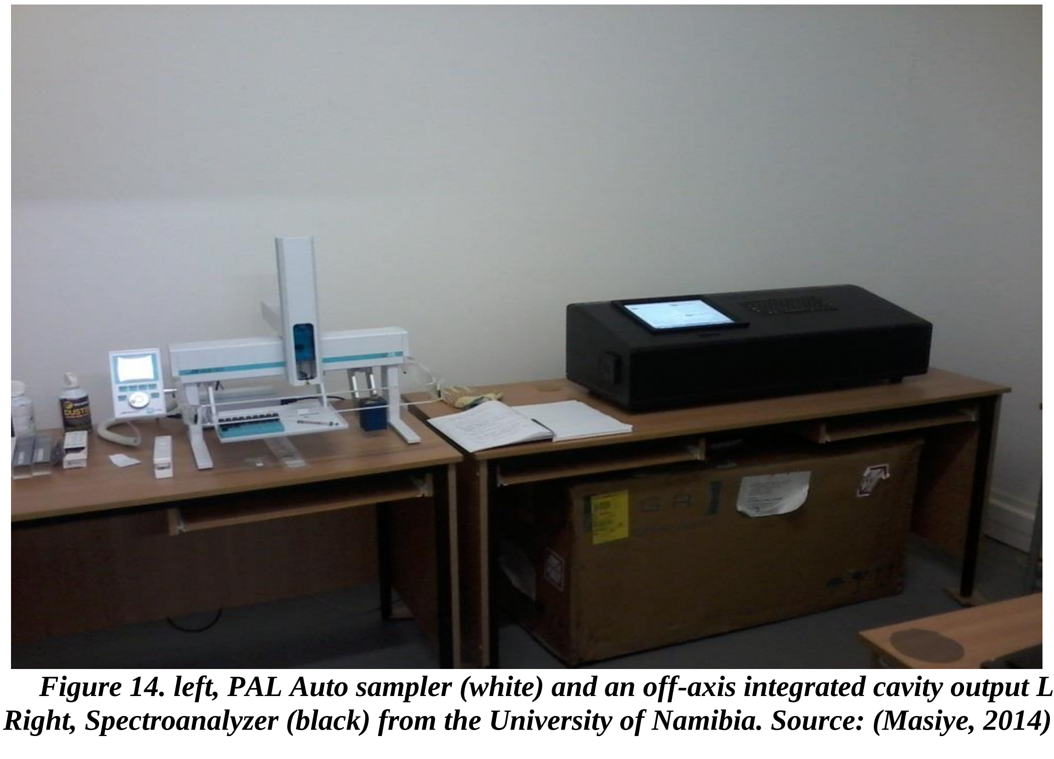

Figure 14. left, PAL Auto sampler (white) and an off-axis integrated cavity output Laser Right, Spectroanalyzer (black) from the University of Namibia. Source: (Masiye, 2014)

4. Results and Interpretation

4.1 Stable isotope

Table 1, 2, 3 and 4 in appendix documents raw data obtained over four different sampling campaign respectively CEB surface water collected for the rainy season 2017. The tables are recording the stable isotope compositions and standard deviations of $\delta^{18}O$ and $\delta^{2}H$ with complimentary characterizing parameters (pH, turbidity, electrical conductivity) per sample. The results are however separately considered per sampling campaigns as shown in most analysis for the account of the temporal variation. Individually the four sampling campaigns (February, March, April, and May) presented different ranges and mean values for the measured parameters. The mean values for the stable isotope composition varied as shown in figure 12, presenting the variation of both $\delta^{18}O$ and $\delta^{2}H$ with time in monthly series. The Box whisker plot (Figure 15) shows that the stable isotopic composition ($\delta^{18}O$ and $\delta^{2}H$) of the CEB surface water varies with time. February had a range of -9.02 to -2.26‰ (mean =-3.65‰) for $\delta^{18}O$ and -65.88 to 7.18‰ (mean = -23.64‰) for $\delta^{2}H$ which relatively shifted to more negative values in March. March range is -13.51 to -5.78‰ (mean = -10.86‰) for $\delta^{18}O$ and -100.08 to -41.47 (mean= -79.74‰) for $\delta^{2}H$. A subsequant positive trend however is shown from March through to April. April ranged from -8.14 to -3.62‰ (mean =4.85‰) for $\delta^{18}O$ and -8.14 to 3.62‰ (mean= -46.78‰) for $\delta^{2}H$. May prsented a range of -6.13 to 12.44‰ (mean = 2.56‰) for $\delta^{18}O$ and -58.2 to 50.93‰ (mean = -0.96‰) for $\delta^{2}H$. Overall the stable isotope composition of the CEB surface water range varies then between -13.51 to 12.44 ‰ for $\delta^{18}O$ and -100.08 to 50 .92 ‰ for $\delta^{2}H$ from Februry to May. Temporal distribution and evolution of the data is further presented graphically in figures 16, 17, 18, 19 and 20, each representing a different comparison.

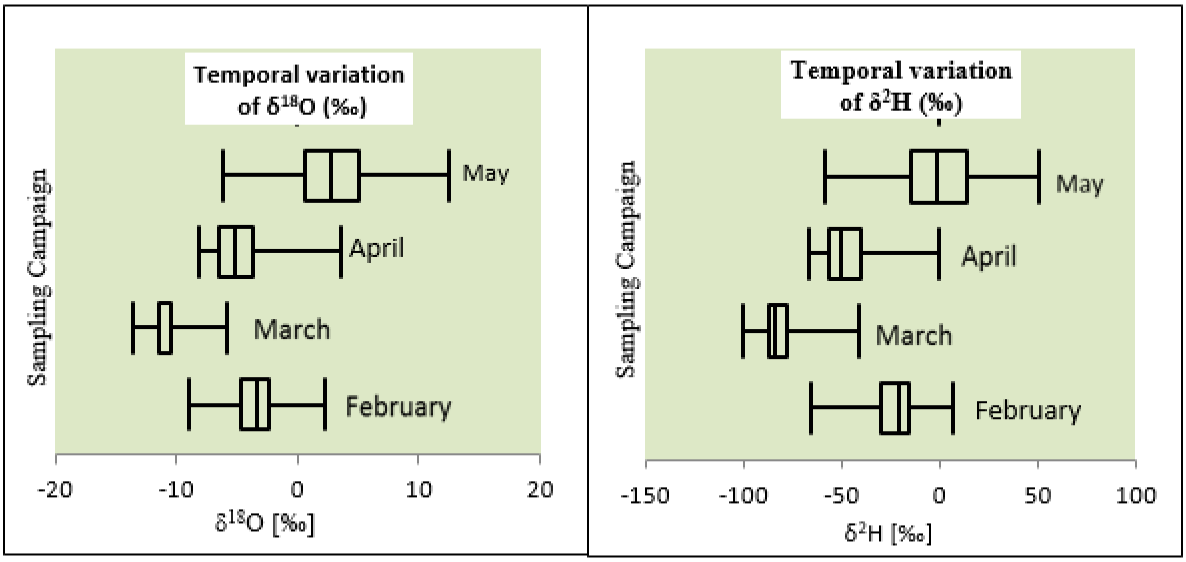

***Figure 15. Box whisker plots showing the variation of the $\delta^{18}O$ and $\delta^{2}H$ over the four sampling campaign respectively*.**

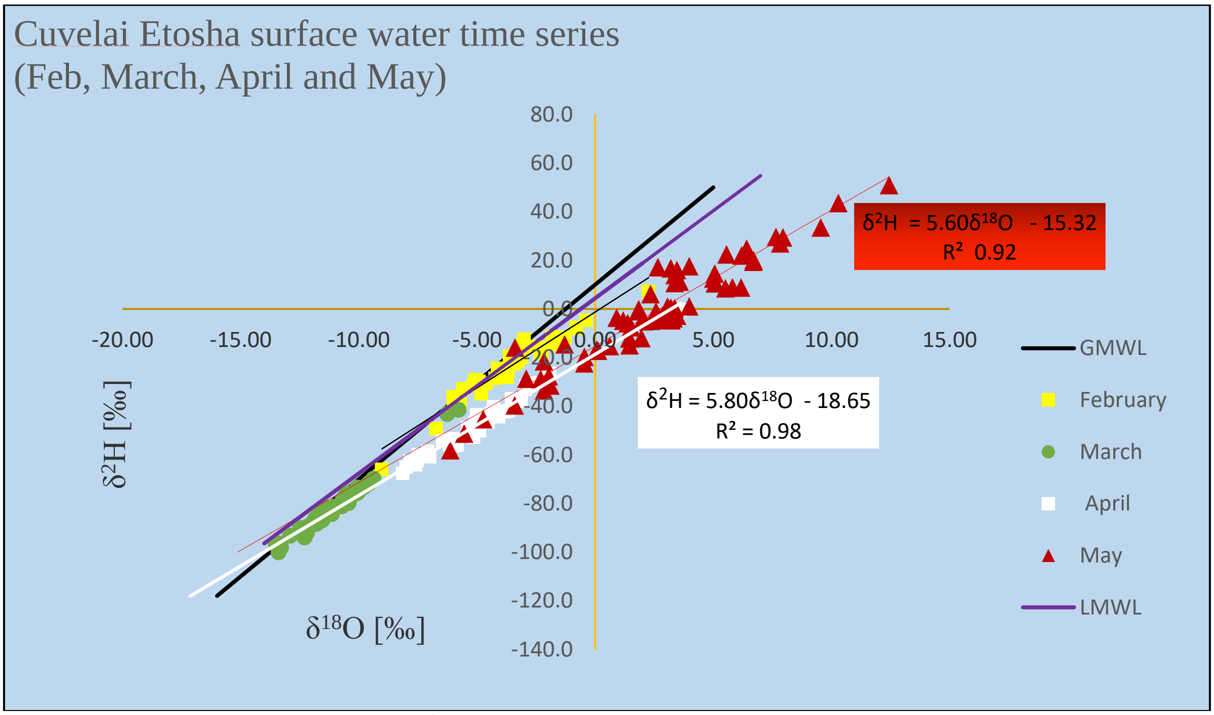

Figure 16. A dual isotope plot of $\delta^{18}O$ vs $\delta^{2}H$ showing the evolution of the CEB surface water through time over four months (February, March, April, and May).

Figure 16 represents data plots ($\delta^{18}O$ and $\delta^{2}H$) with respect to the GMWL and LMWL as a function of time. Each color code represents a different sampling campaign. The data plotted clusters of points per sampling campaign with overlapping seen between some campaigns. Data collected in February which represent initial precipitation with negligible evaporation events plots perfectly on the LMWL and tightly close on the GMWL but few offsets are also common. The offsets from the meteoric water lines (MWL) can be attributed to water that had undergone evaporation. (Plata, 1994) as cited in (Andreo et al., 2004) documents such plotting to result from evaporation either in the lowest part of the cloud, during its route towards the rainfall site or to the partial evaporation of the water drops before their arrival at the land surface. In additional to the stated processes, minimal evaporation of the water while on the ground which most likely occurred prior to sampling can also contribute to the offsetting of the data plots. The majority of data points for the February sampling campaign however plots perfectly on the MWL. This directly indicates a similar meteoric and vapour source as those represented by the GMWL and LMWL. The range -9.02 to -2.26‰ (mean =-3.65‰) for $\delta^{18}O$ and -65.88 to 7.18‰ (mean = -23.64‰) for $\delta^{2}H$ for february can be used to represent the isotopic composition of CEB surface water prior to the incoming of the Angolan flood water. The regression line plotted from February data is

$\delta^2H = 6.24\delta^{18}O - 1.25$ with $R^2 = 0.94$ (n=58)

Compared to the equation for the CEB precipitation, $\delta^2H = 7.2\ \delta^{18}O + 4.4$; $R^2 = 0.99$ (Turewicz, 2012) and that from (kaseke., et al 2016) , $\delta^2H = 7.1\ \delta^{18}O + 1.6$; $R^2 = 0.97$ derived by kringing vs , $\delta^2H = 8.2\ \delta^{18}O + 13.9$; $R^2 = 0.94$ using globally fitted isoscape (GFI) modelling (Figure 8). It has the smaller slope and a lowest d-excess. This was expected due to differences in residence time of exposure to the CEB environment and thus variance subject to disequilibrium hydrological operatives on the isotope composition. The February data plots do not represent precipitation even though it was the only input to the surface water system at the time. More over the regression line is a reflection of the ground influencing processes with evaporation being the most likely composition controlling processes. The equation for the CEB precipitation is expected to change with time with slope close to 8 for as long as the source origin does not change.

The March data plotted in green (figure 16) shows a shift down the water lines representing a depletion in the isotope composition. The range has then change to more negative values as presented by box and whisker plots in figure 12 with ranges -13.51 to -5.78‰ (mean = -10.86‰) for $\delta^{18}O$ and -100.08 to -41.47 (mean= -79.74‰) for δ^2H. This period captures peak flash flood inflow and rainfall and thus suggests both the amount effect and the Altitude effect. Summer rainfall events of the CEB are at peak rates during February-March. Similary the inflow of the flood water will then also result in the same shifting of the isotope composition. The inflow flash water are from high amount events events, sub tropical part of the Cuvelai (the Angolan part) and from a relatively elevated area. collectively the amount effect and the altitute effect then influence the composition of the CEB surface water during March. Relatively an increase in isotope composition value thereon from March to May is shown by the April and May data clusters. The May and April data plots elliptical data clusters below the GMWL and LMWL with notable overlapping compositions. The overlapping is an indication of progressive enrichment in the CEB surface water and can be attributed to one or groups of ground level effects on the isotope composition. Similarly the two data clusters (April and May) shows typical plotting of evaporated water on the dual isotope scatter plots. Comparatively however the May data relative to the April plots to more enriched values and further away down the GMWL in a more scattered data distribution pattern. The scattering is attributed to the onset of locally focused ground condition as compared to March and April data with more homogeneous influence across the studied area. Close clustering March and April data points is influenced by dominantly influencing high volumes of the flood water. This high volumes has the potential to overpower locally focused contribution on the isotope composition alteration. Overlapping is noted between the Aprils and May data despite both plotting regression lines with slightly different slopes.

The April data plots a regression line

$\delta^2H = 5.80\delta^{18}O - 18.65$ with an R^2 of 0.98 (n=43)

This regression line represents an evaporation line for the CEB surface water during the April month 2017 and intersects the GMWL at (-12.73‰ δ^2H, -91.84‰ $\delta^{18}O$). This composition is within the range of isotopic composition recorded for March. The slope is slightly higher than for a typical semi-arid country but to a strict sense, the slope is easily influence by several factors. Collectively the slope of an evaporation line is a function of humidity, air temperature and wind which may vary locally causing variation even between countries of similar climatic conditions. Further proving the effect of evaporation on the isotopic composition are the results from samples collected in May.

$\delta^2H = 5.60\delta^{18}O – 13.32$ with an R^2 of 0.98 (n=66)

The regression line for data collected in May has slightly a lower slope than that for April which points to a better representation for a typical semi-arid country. The difference in the number of entries in the dataset (n) could also be used to translate to better presentation of local system 66 vs 43 for May. But more over differenced in the slope can be attributed to a change in relative humidity.

Furthermore a comparison is made between water collected from Angola with those from the Namibian Cuvelai counterpart during the same time (February and March) as shown by figure 17. Overlapping is persistently observed with points plotting predominantly on the GMWL and LMWL through both months. The overlapping suggest common storm events, which is most likely due to close proximity of the sampled areas. The maritime vapor sources may be the same for both areas and/or the environmental controls imposed on the isotopic composition may be similar at that time in space. A common shift towards more negative values is evident on both sides of the Cuvelai system with the Namibian stretching slightly furthest down the GMWL. This signature to a subtle consideration points towards more depleted water on the Namibian counterpart during the month of March. The density of data however plays a role on what is to be statistically concluded on and thus the small data density seen for the stretch could be a limitation to true reflection of the measured attribute.

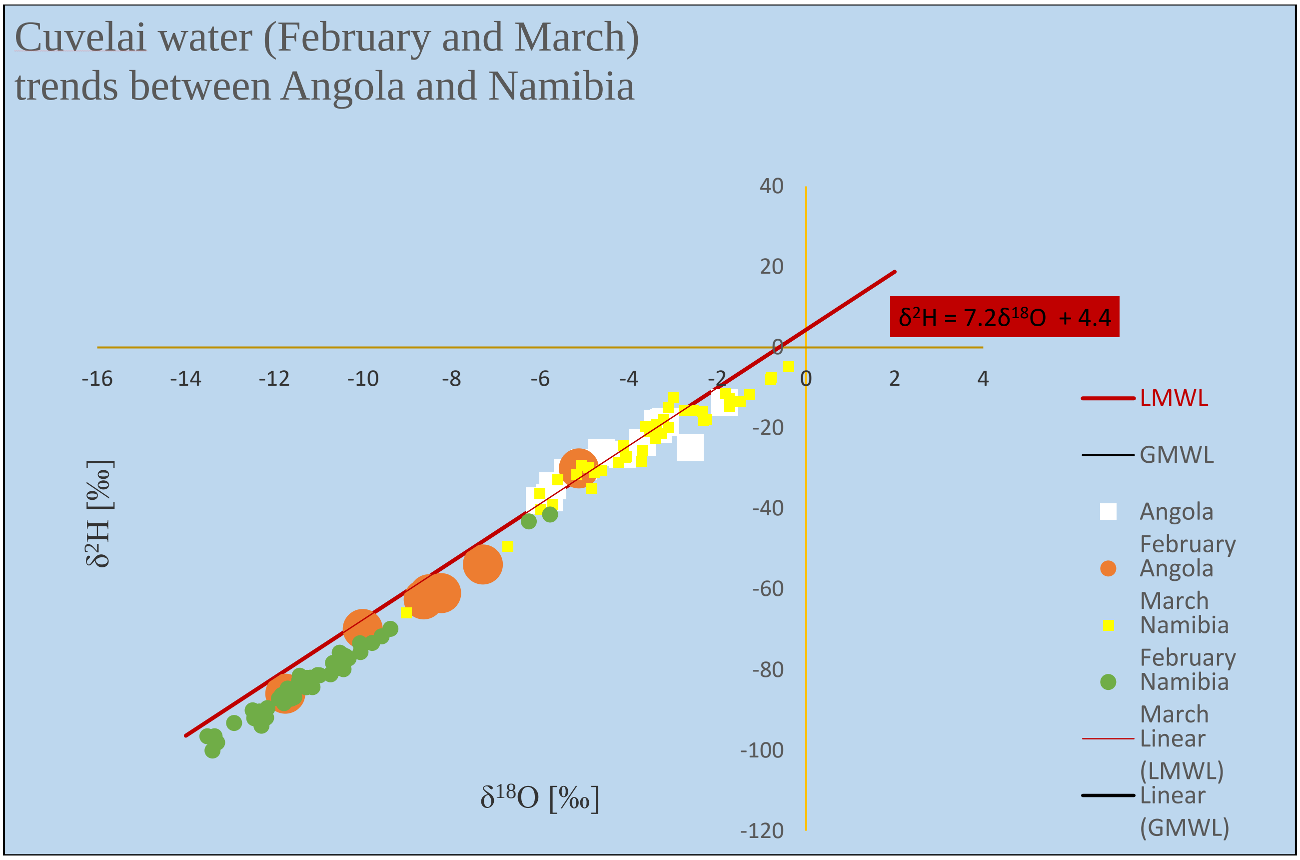

Figure 17. Spatial and temporal trends (comparison between Angola and Namibia water on time series).

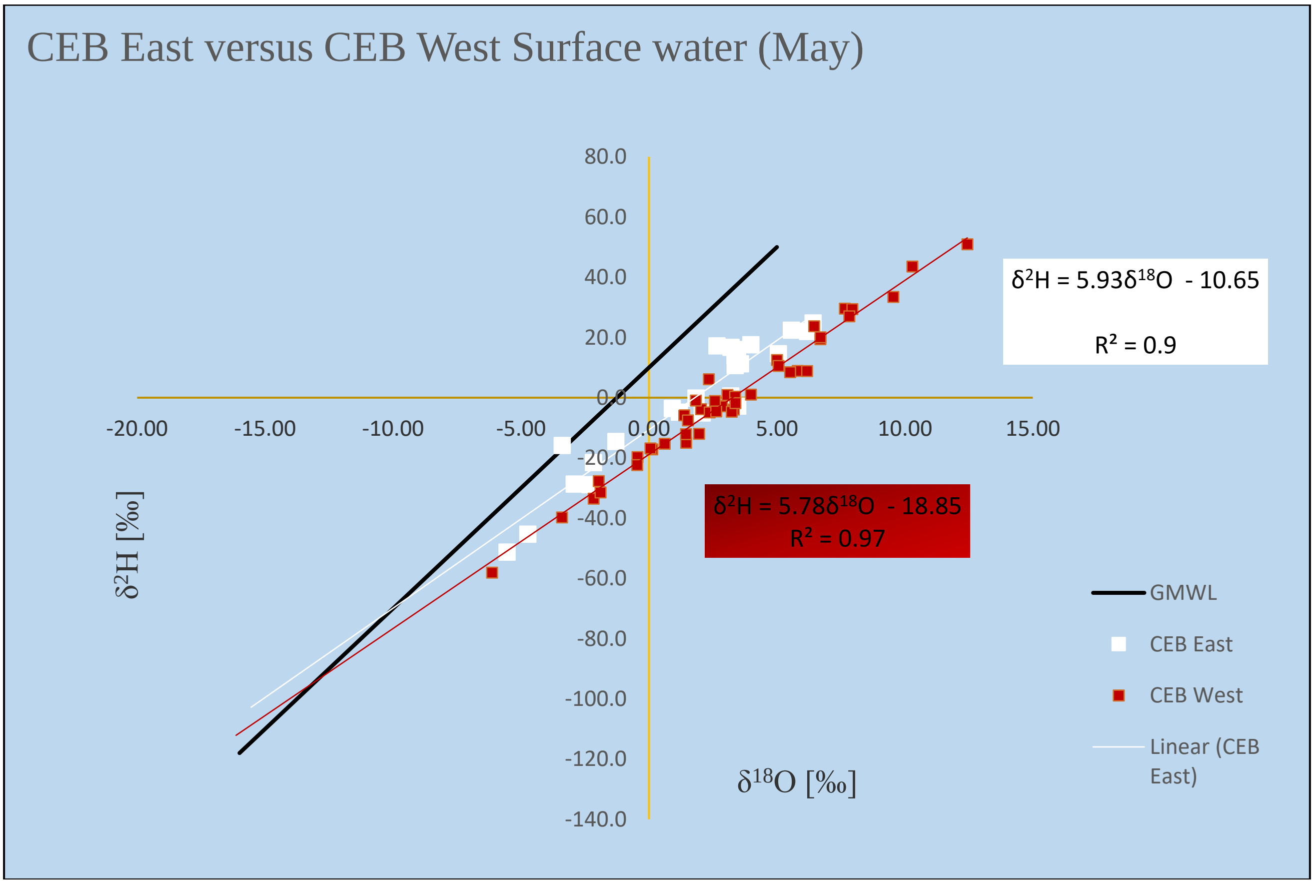

Figure 18. Spatial trend (comparison between the east and west part of the CEB).

A north-south spatial comparison (Figure 17) per sampling campaign shows no significant differences in the isotope composition in that transect. This poor relation is attributed to a limitation related to the studied area scale or due to limited samples collected on the Angolan counterpart. Similarly an attempt to understand spatial trends in the east-west direction was possible with data collected in May 2017. As shown in (Figure 18) both data sets predominantly plots sub parallel linear distributions of points below the GMWL. The results shows similar range of isotopic composition for both east and west although the west data plots furthest away from the GMWL. Linear regression lines with strong correlations are realized from both data set respectively and intersected the GMWL at two different positions. The CEB West water regression line intersect the GMWL at more negative values (-13‰ $\delta^{18}O$; -94‰ $\delta^{2}H$) of isotope composition relative to the East (-9.98‰ $\delta^{18}O$; -69.84‰ $\delta^{2}H$). This then suggests that samples collected from western parts of the CEB has a source or a major source influencing event that is predominantly more negative than those from the eastern part. The slope of the regression line representing water from the CEB east is slightly higher than that realized from the CEB west. This pattern is aligned with the findings from (kaseke., et al 2016) in that the relative humidity increases easterly. The higher relative humidity samples in the eastern part of the CEB presented an evaporation line with an equation with a higher slope as compared to the CEB west surface water. Stable isotope composition results from the 2017 sampling campaign as compared to the 2014 sampling campaign taken at the same time of the year shows significantly distinct range of compositions (Figure 19). The evaporation line for the 2014 data has a lower slope of 4.88 while that for the 2017 is 5.91 and the difference is linked to differing environment conditions such as the relative humidity. The two lines intersects the GMWL at two distinct positions, with the 2017 water displaying an intersection at more depleted isotopic composition values of -12.52‰ $\delta^{18}O$ vs -90.16‰ $\delta^{2}H$ as compared to -7.15‰ $\delta^{18}O$ and -47.2‰ $\delta^{2}H$ for the 2013 CEB surface water. This difference implies the source water for CEB surface water for the year 2017 was more depleted as compared that of the CEB surface water in 2014. 2017 year had a more intense flood as compared to that of the 2014 and thus the more depletion in heavy stable isotope in 2017 CEB surface water.

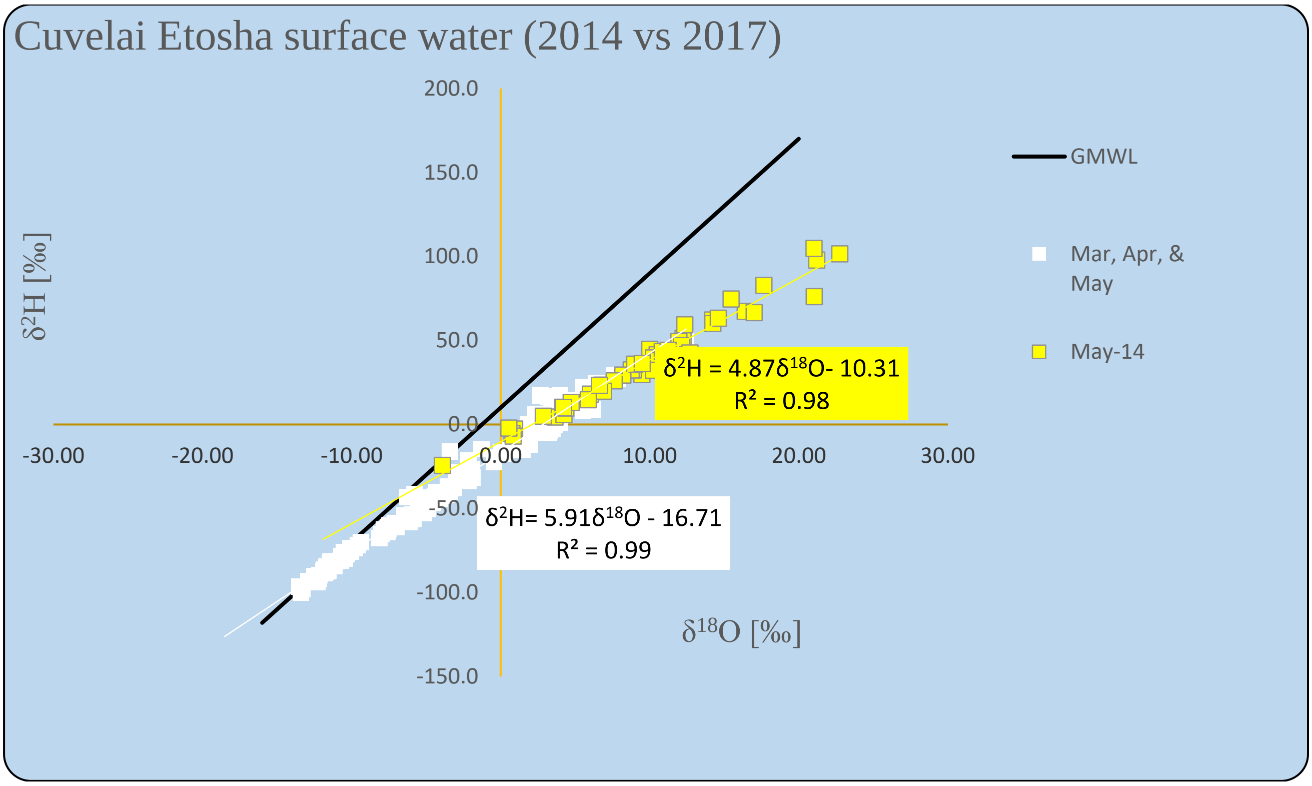

Figure 19. Temporal trends (May 2014 vs 2017) for the CEB.

Appendix table, 1, 2, 3 and 4 shows arithmetic average D-excess on monthly series (February, March, April and May) for the CEB surface water. D-excess is a good discriminatory for the precipitation water as it can be used as fingerprint of (1) the oceanic source area of the precipitation collected at a given station and (2) mixing of air masses of different source, in particular, recycled air moisture (Frohlich et al., 2002). The application of D-excess can be carefully applied to surface water to access the source and subsequent processes that effected its isotopic composition. February had an average value of 5.56 ‰ and captures initial precipitation without flooding or severe evaporation. Several sites however measured a D-excess close to 10‰ during the first and mostly during the second campaign. This value directly translates to Atlantic or Indian ocean as the source. The source was better represented by a mean of 7.1‰ obtained for the march month. April and May month both records reduced and negative value for D-excess, -7.99 and -11.48‰ respectively. D-excess is reduced in the case where water is lost by evaporation (Frohlich et al., 2002) during raindrop. The effect is even further emphasized under severe ground evaporation like that of CEB conditions. The D-excess therefore further proves the effect of high degree of evaporation on the CEB surface water stable isotope composition. Comparison on a regional scale by using data compiled by (Turewicz, 2012) demonstrated the importance of describing isotopic data in time series. Figure 20 compares the stable isotope composition of various surface water collected at different places in Namibia and across its borders for a spatial comparison. Namibia surface water systems reported for this study wholly ranged between -13. 9 to 5.19‰ for $\delta^{18}O$ and -100.08 to 22.17‰ for $\delta^{2}H$. There exist distinctions in the isotopic composition however which may then vary with time as demonstrated by the CEB surface water data. The change with time is attributed (as demonstrated by the present study) to hydrologic events collectively affecting the water per time in space. Other areas beside the CEB data, are not recorded in time series and therefore represent compositions per one time of sampling and therefore are indicative of absolute compositions than ranges. Collectively Perennial rivers systems of Namibia (Okavango, Kunene. Zambezi River) plots similar compositions between -5. 26 to -1.73 ‰ for $\delta^{18}O$ and -40.04 to 14.6‰ for $\delta^{2}H$ which is indicative of similar storm events and/or subsequent environmental effects. Orange River water collected from Upington (South Africa) however reflects more enriched values -1.63 to -1.08‰ for $\delta^{18}O$ and -5.77 to 4.55‰ for $\delta^{2}H$. The differences is a reflection of differences in the geographical positions and thus differing environmental controls on the isotope data. Upington surface water is found more inland, at more elevated terrain, the reverse of the determined range results are expected due to the rain out effects. However depended on the source water, land elevation, storm intensity, Evaporation severity, and seasonality of precipitation (summer or winter), rainout effects can be counter played. Upington receives summer rainfall just like Namibia (https://www.yr.no/place/South_Africa/Northern_Cape/Upington/statistics.html) and thus the enrichment is most likely to be due to altitude effect. The origin of the river is about 3300m above sea level and possibly due to high evaporation severity and the same is seen for Kunene River.

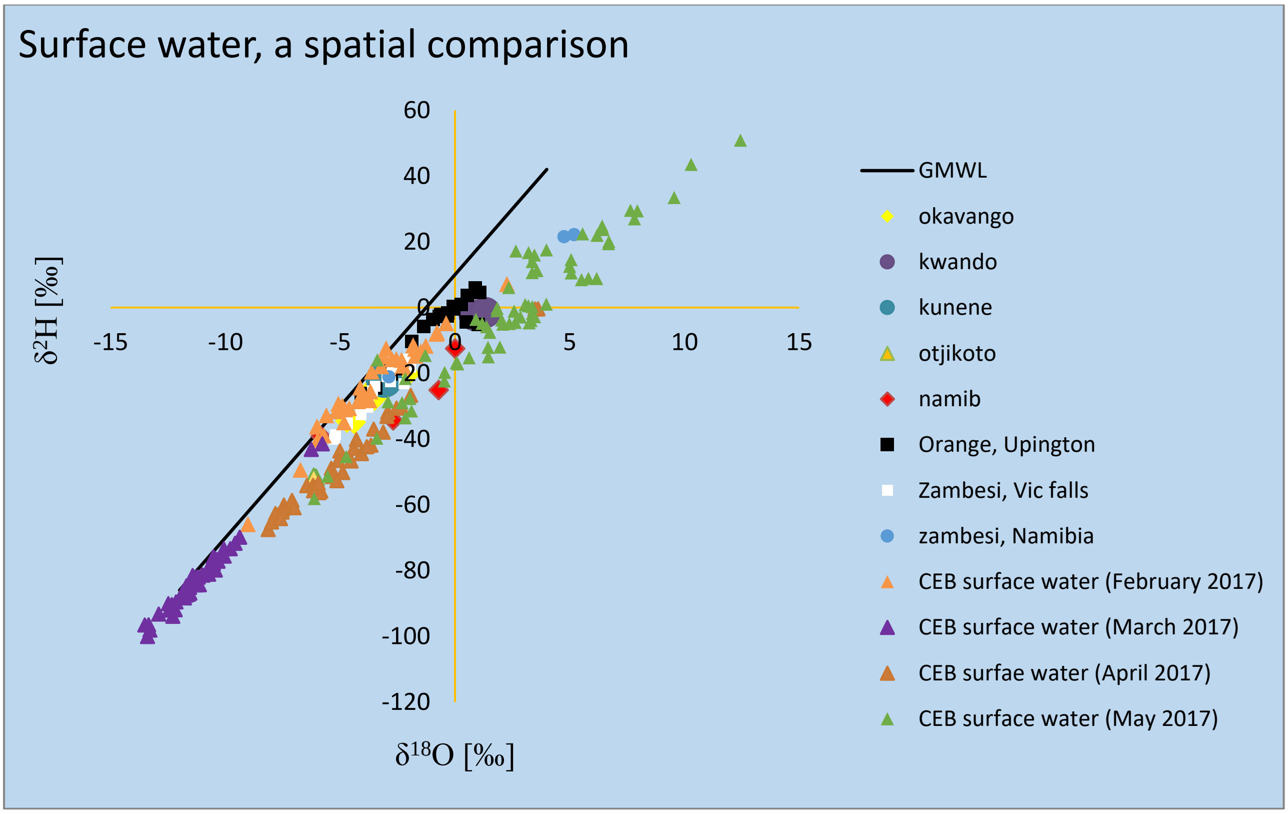

Figure 20. Regional comparison of Surface water in southern Africa.

An attempt to correlate the isotopic composition ($\delta^{18}O$ and $\delta^{2}H$) for other catchment effects was considered. Isotope effect to changes in elevation, distance from the ocean (longitude) and latitude for spatial variations are common for hydrologic studies of catchments. The degree of correlation however in those aspects were not significant, very small $R^2 < O.2$. This poor to none existing relation can be attributed to the study area scale limitations. The sampling sites had similar elevations ranging between 1094 and 1118 meters above sea level and a low topographic gradient. A reflection for the altitude effect on the isotopic requires a significant difference for the sampled sites. The longitude effect study was limited by the scale of study as it was concentrated on the Cuvelai drainage zone and thus mostly in the west part of CEB. Samples collected in the West and East part of the CEB after flash flooding events had significant differences in the stable isotopic composition ($\delta^{18}O$ and $\delta^{2}H$). The difference however is attributed to the strong influence from the flood water rather than the differences in the longitude. This relation is then seen to oppose the inverse relation between the distances from the coast and the stable isotope composition as theoretically defined by (Dansgaard, 1964; Andreo et al, 2002). Differences in the latitude of the study area was rather small to reflect effect on the isotopic composition and thus a poor to non-existing relation between latitude of sampled areas and stable isotopic composition ($\delta^{18}O$ and $\delta^{2}H$) was presented.

4.2 Physio-chemical parameters

Complementary characterising parameters were measured along with the isotopic composition throughout the sampling campaigns in year 2017. Results are summarised on the box whisker plots for the electrical conductivity and the Ph in Figure 21. The electrical conductivity for the CEB surface water range changes with time as revieled by shifts of the boxes. Overall throughout the four months the electrical conductivity ranges between 0 µS/cm and 776 µS/cm. The 3rd quantile does not significantly change with time for the first sampled three months. The minimum of the electrical conductivity thoroughout the four sampling campaigns does significantly change as compared to the maximum. The maximum bounds are often occuring as outliers and thus far from the 3rd quantile for all sampling campagin. Collectively then using the 3rd quantile as upper limits, the CEB surface water electrical conductivity dominantly range between 3.12 µS/cm to 238.75 µS/cm but however higher values of up to 776 µS/cm were encountered on rare cases. The highest electrical conductivity is within a range of data points collected in April. April accounts for a span of evaporation exposure and thus the increased levels in electrical conductivity could be linked to enhenced evaporation influence. The pH as seen in (figure 18) is similarly sensitivity to hydrological activities as shown by shiftings of the whisker limits captured by the different sampling campaigns. In February the pH varies between 6.64

to 9.09 and a slight change to lesser range bounds is seen for march. April records the more less pH range of 5.14 to 7.7 whilst in May the pH varies between 5.96 to 9.2. Overall the values of the CEB surface water over the rain season as recorded from February to May dominantly varies between 5.78 to 8.6 while extremes values such as 5.15 and up 9.27 were locally encountered on rare cases. The variation in the initially determined by local focus processes in early months. The shifting to lower values can be attributed to mixing of different waters or dominance of further precipitation water . The increased in the ph is consistent with the increase in the degree of evaaporation thus evaporation could be the process elevating the ph to higher alkalinity.

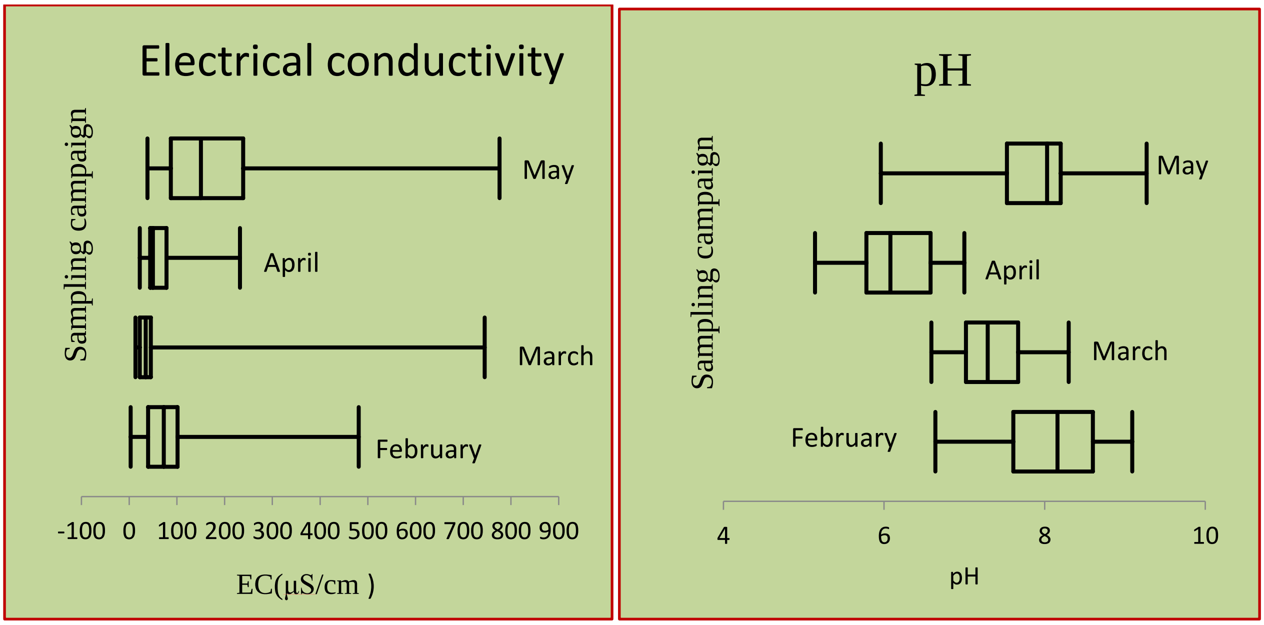

Figure 21. Measured pH and electrical conductivity results.

Selected samples based on electical conductivity targetly within low, medium and high levels were analysed for the chloride content. Chloride content results plotted against electrical conductivity from samples collected from different sampling campaigns is shown (Figure 22). Scattely distributed data with a very low linear relationship (R^2 =0.11) is shown by data from february. February captures samples from initial precipiation with negligible evaporation and values as high as 103 mg/l for the chloride content is attained. The February data plots scatterly and is indicative of locally focused altering processes. This influence however is minimised by increased water amount as captured by the March sampling results. The positive linear relationship is improved to an R^2 of 0.98 from samples collected during peak precipiation and flooding events (March). The events colectively plots low chloride contents in the range of 6.24 to 16.8 mg/l. Samples collected after severe exposure to evaporation plots a range of a range of 5.67 to 67.9 of mg/l for chloride content. This data shows scattered point distributin with a moderate linear positive relation as revieled by an R^2 of about 0.57.

A temporal relation study between the chloride content (mg/l) and δ^{18}O (‰) show a persistendly similar trend between the two parameters with time (Figure 23). The polyline trend lines as shown shows that a decrease in δ^{18}O (‰) is accompanied by a decrease in chloride content (mg/l) and vice versa. Increase trends are consistend with the degree of evaporation and offsetting of further water inflow into the system. The direct translation is that the processess affecting the δ^{18}O (‰) similarly affects the electrical conductivity.

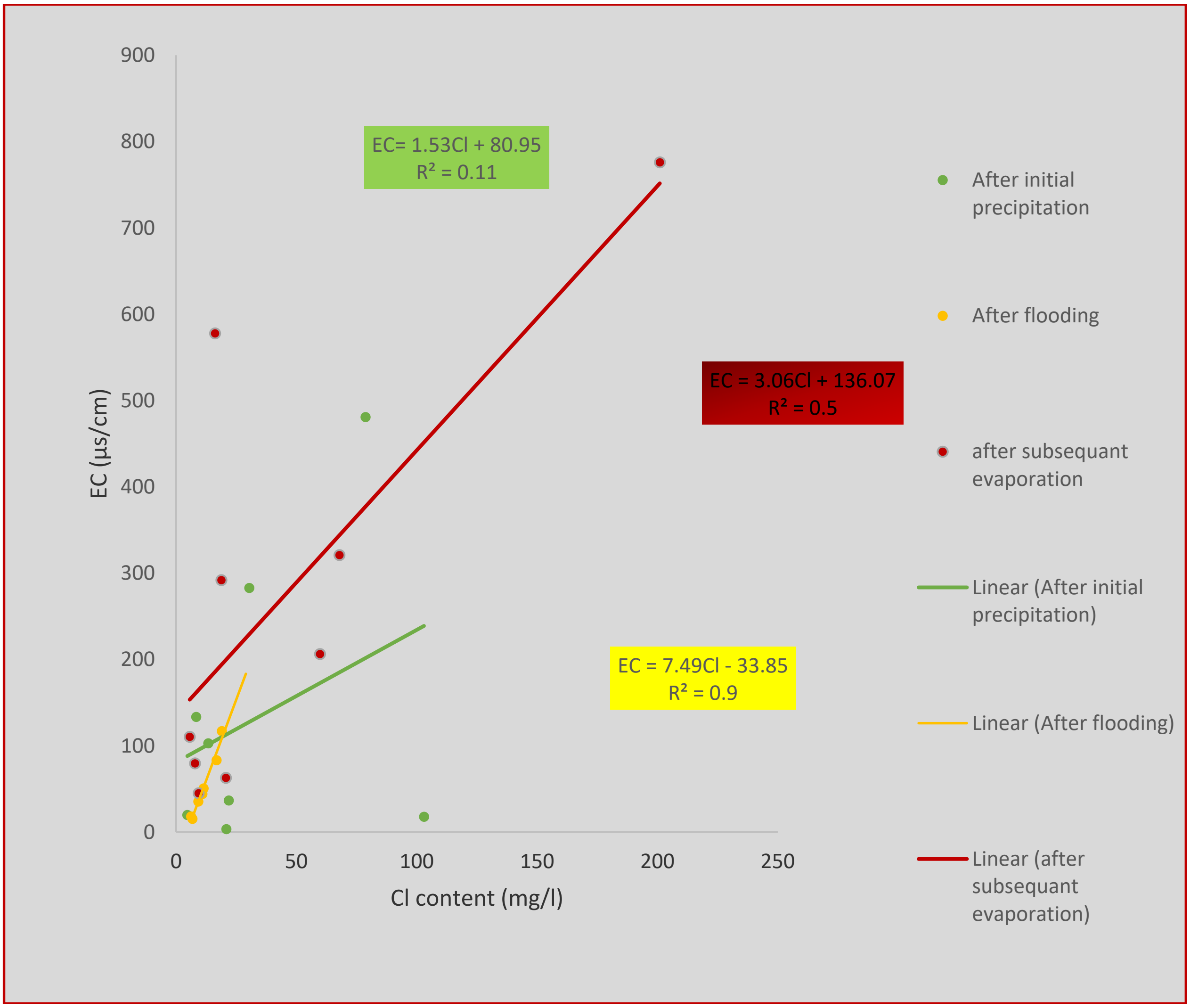

Figure 22. Electrical conductivity versus chloride content from various sampling campaign collected in 2017.

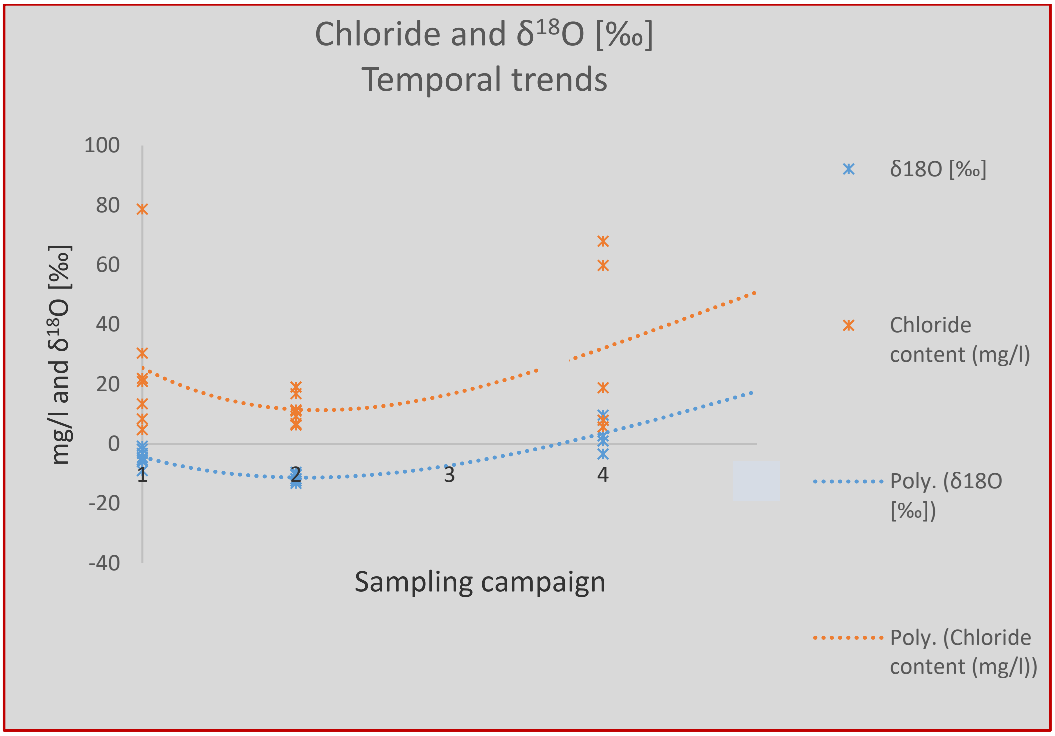

Figure 23. Electrical conductivity, δ18O [‰] variation with time. From various sampling campaign collected in 2017.

Turbidity mean results, reported in (FAU) considered from samples collected during the 2017 sampling campaigns are presented in (figure 24). The mean calculation excluded those that had turbidity above the equipment detection limit (1110 FAU) for absolute value analysis. The exclusion aimed to obtain absolute estimate for turbidity values, existence of turbidity above the electrode detection limit is however considered during interpretation. Notably the mean for turbidity varies similar to the stable isotope composition of the water. A decrease from February to March and thereon an increase from March to April. The similarity can exist because turbidity is then a function of constituents in the water, energy of the water system and volume of water. For as long there are processes or events that are effecting any of the above factors which are also alters the isotope composition, similar trends may be realised. The trend is described as an increase in turbidity with time and therefore becomes a threat and a subject to the quality of the surface water. This indicate that there will be time that the CEB surface water will be unsuitable for human and livestock consumption due to parameter “turbidity”. Similarly, when turbidity is classed, the frequency per sampling campaign as shown in (Figure 25) points to the same threat. Class 200-500 dominates from February, March through to April and attains the highest dominance (80%) in March. March and April records peak precipitation and flooding events, which are events that can be possibly linked to high dominance in low turbidity classes as compared to the high ones. The pie frequency chart for the May data reveals highest dominance (35%) from class 1110-1400 as compared to the usual leading class (200-500). This change can be described as a relative increase in turbidity from March to April, a trend which is consistent with reduced precipitation amounts and on setting of evaporation events. The class has no upper bound defined and no absolute values can be provided which can virtually translate to only a deterioration in the quality of the CEB surface of water with time. The exact value of turbidity threat however could not determine by the used equipment for the present study due to detection limit. On average the CEB water scores a class 4 according to the Namibia water standards. A worsening threat to the quality of CEB surface water figure 24 and figure 25 reveals a worsening threat to the quality of the water regarding parameter “turbidity”.

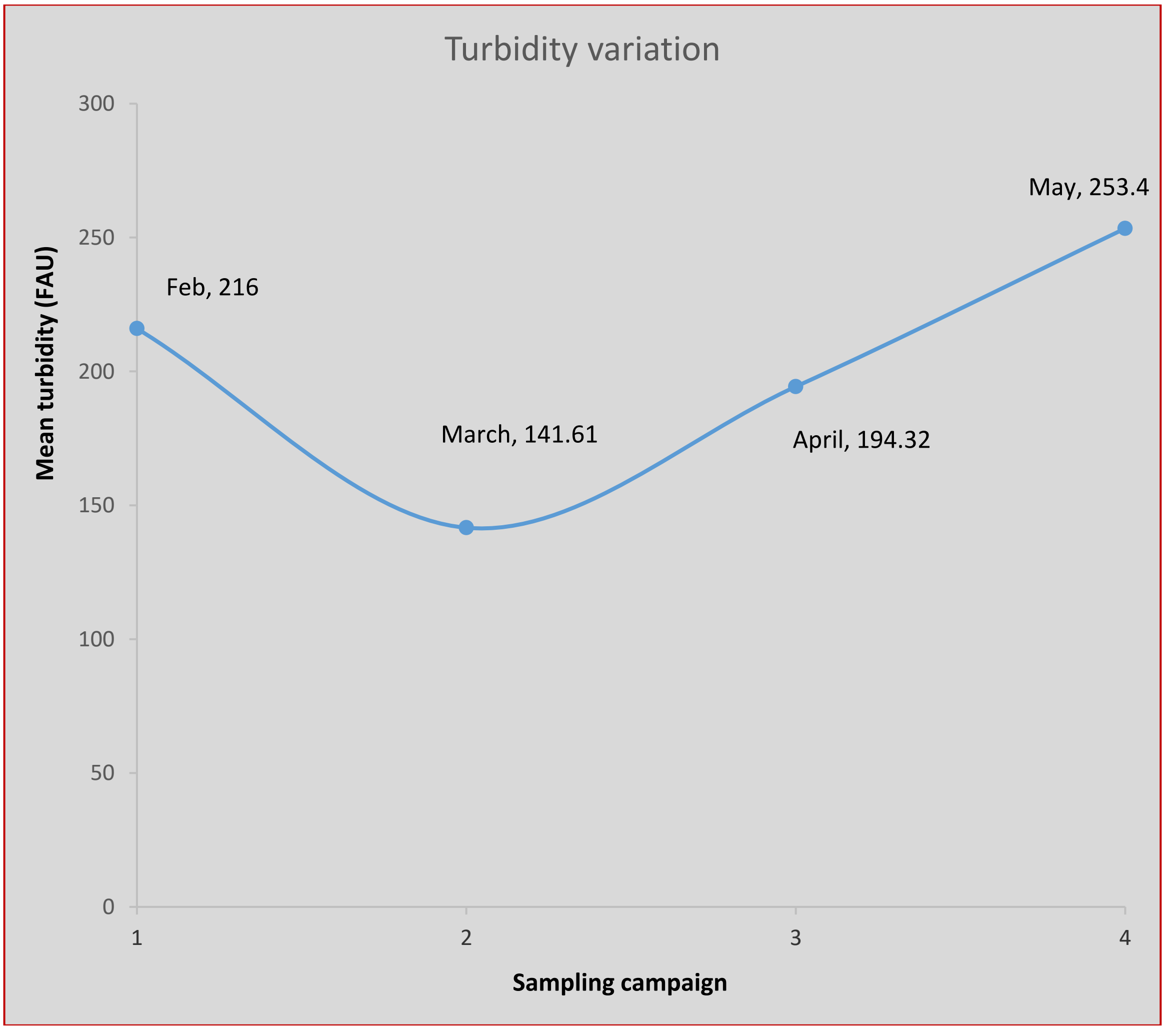

Figure 24. Mean turbidity calculated on month time series from February to April.

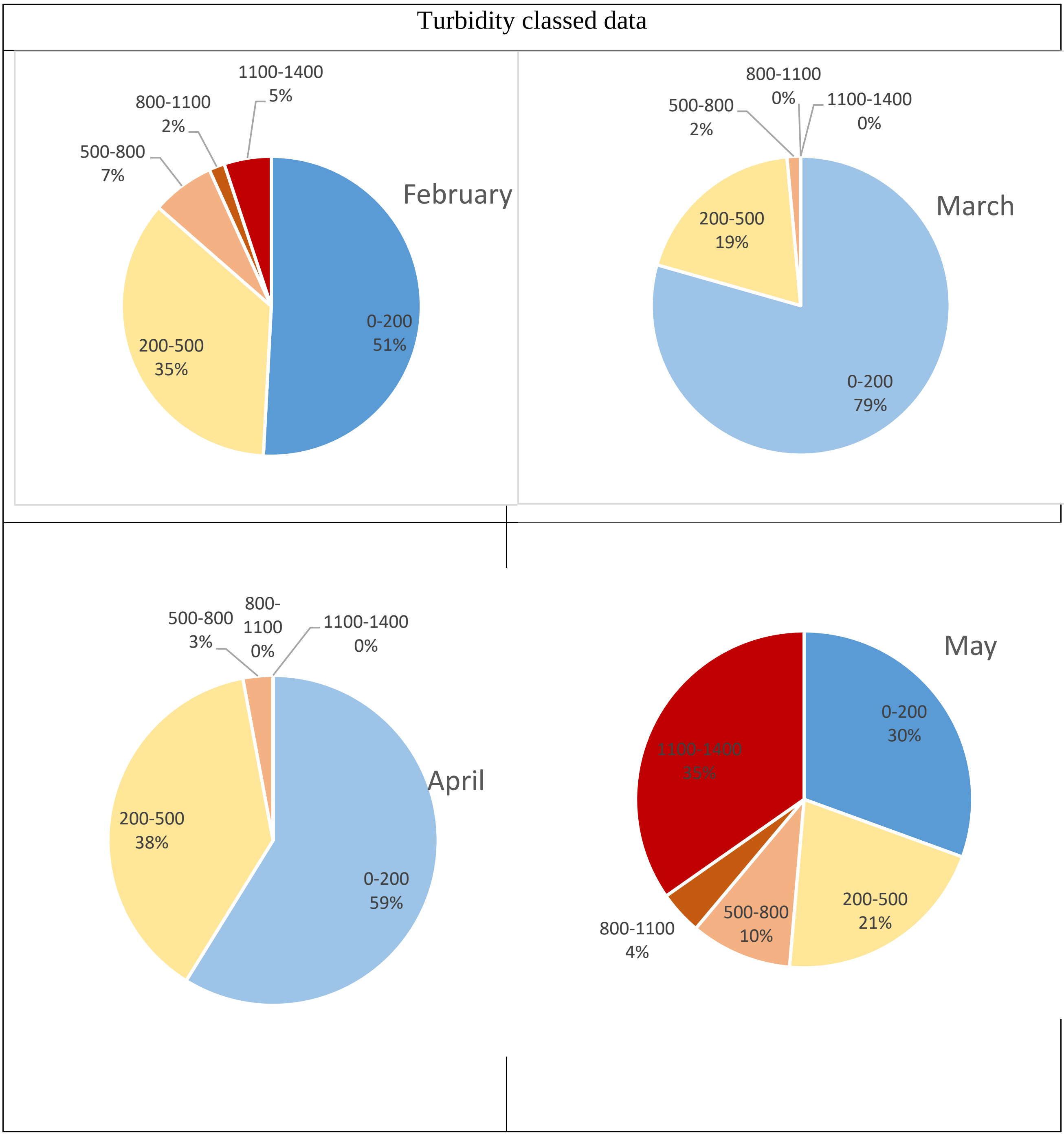

Figure 25. Frequency pie chart for turbidity result per sampling campaign.

5. Conclusion

There exist mappable temporal variations in the stable isotope composition of CEB surface water. This trends are mainly reflections of the inflowing flood water, differences in precipitation amount and degree of evaporation influence with time. Peak stable isotope compositions in the CEB area are consistent with peak hydrological events affecting the CEB surface water system such as flood, precipitation and severe evaporation. Overall the stable isotope composition of the CEB surface water range varies between -13.51 to 12.44 ‰ for $\delta^{18}O$ and -100.08 to 50 .92 ‰ for $\delta^{2}H$ from Februry to May. The overlapping seen for the earlier sampling campaigns concludes to a common storm on both side of the border (Angola/Namibia). Both sides receives precipitation from common storm events atleast on the measured scale. Comparatively the Angolan water may be isotopically depleted due to the altitude effect and the amount effect. Along with the altitude effect, the amount effect also took its toll on the CEB surface water and depleted the water to more negative compositions. The present study demostrated that the stable isotope compositions are time depended parameters. Conclusively, Similarities and differences in hydrologic events and interaction can be revealed using stable isotope composition and may change with time or climatic condition. CEB east surface water are less influenced by flood as compared to the western part, giving rise to the only spatial trend identified by the present study. This spatial trend does not directly translate to any of the so called isotopic effects but rather due to mixing of CEB precipitation water with the flood water. Active circulation of flood water which is dominantly to the west part of CEB depletes the surface water stable isotopic composition ($\delta^{18}O$ and $\delta^{2}H$)‰. Under current climatic conditions, similar isotopic compositions are therefore possible across the western to the eastern areas given an absence of flooding events. Spatial trends in the CEB are most unlikely to show on a south-north transect due to scale limitation. Spatial trends on a larger scale (whole cuvelai scale), may be mappable. This trends may be induced by the differences in the amount of precipitation, change in elevation. and largely also due to change in latitude. Conclusively the isotopic composition of the CEB owes its shifting to negative extremes to the amount and altitude effect through the flood water inflow from Angola. Consequentially, the CEB surface water stable isotope composition is modified progressively to more enriched values after the cease of flooding and rainfall events. No latitude effect, altitude effect and continental effect were identified for the CEB surface water. A relatively high evaporation slope for a semi arid country like namibia was determined by the present study. The high evaporation line slope is attributed to a relatively high relative humidity during the wet season. Increased relative humidity in the eastern part influences the evaporation slope to even higher value. Therefore the slope of the evaporation line decreases with the degree of evaporation which is in turn a reflection of the change in the relative humidity. Several samples have pointed to the Atlantic and Indian Ocean as the maritime vapour sources for the CEB precipiation. Differentiating of source vapour masses is a complex subject due to the geographical position of Namibia with respect to the sorrounding expanse of oceans. A realisation of such discrimination will require precipitation samples rather than surface water sample for a better estimation. The same hydrologic operatives effecting the stable isotope budget can inturn also alter other physio-chemical parameters and thus should be individually monitored. pH and electrical conductity are no areas of concern pertaining to the quality of the CEB surface water unlike parameter turbidity. According to the (WHO) 2011 standards, the CEB surface water pH and electrical conductivites are within safe ranges for human consumption, domestic use and agricultural use. Measured turbidity levels however identified a detereoration of the quality of water with time. Turbidity is a concern due to possible microbial contamination alarms a threat to management in providing safe water to the communities of the CEB. The etablished characterising baseline data on temporal and spatial scale now can serve as a proxy for practical use in the hydrology, hydrogeology, forensic and ecological studies pertaining to the CEB.

6. Recommendations

Stable isotope composition are very responsive to changes in climate and processes effecting the water systems. The present study has demonstrated how the composition may change with time depended on the hydrologic operatives. The usage of stable isotope data should therefore be time based to avoid false interpretation and understanding of systems. Despite the evolution of surface water the variations however plots finite ranges of composition, and may therefore be mapped into characteristic signatures of the basin. Data measured for 2014 as compared to the 2017 has clearly shown how important is to keep a continual measurements of the surface water for a better representation of the system. More and further study of the kind has the potential of improving the database for any usage that might arise in the future. A nationwide mapping of stable isotope of the surface water system is therefore recommedated for a better regional comparison. 2017 sampling campaigns records for a relatively high rainfall with a severe flood. Therefore in the long run, similar studies are recommended to measure the evolution of the surface water during different season experiences of low, moderate or high rainfall and/or flooding severity. The present study did not sample precipitation. The initial composition of the precipitation water for the CEB under current conditions is therefore still not defined on a temporal measure. The evolution of water is better understood and represented for with knowledge of initial precipitation per season. On record In order to decipher the origin of source vapour for the precipitation, there is a need to sample precipitation water. Precipitation water should be sampled across a scale larger than the Cuvelai in order to account for the influence of the source to the spatial distribution of the stable isotopes. Again there is a need to do such kind of study on a time series manner in order to monitor changes in the precipitation regime as a function of time. Spatial distribution patterns on the stable isotopes are less detectable on a small area of coverage, it is therefore recommended that a proper spatial representation to be studied using a larger scale. There is a need to further study turbidity in order to quantitatively measure the threat to the CEB surface water quality by parameter turbidity. Measurements should define safe limits upon which advices to local communities should be based on. Conclusively there is a need for a continual study and timely updating of the isotope data for establishment of robust baseline information for future scientific study in the area.

7. References

Books

1. Clark, I., Fritz, P., 1997. Environmental isotopes in hydrogeology. Abingdon, united kingdom CRC Press. P1-P78.
2. Mays, L.W., 2012. Ground and surface water hydrology. United States of America: John Waley & sons. P1-68.
3. WHO., 2011. Guidelines for drinking-water quality - 4th edition. 20 Avenue Appia, 1211 Geneva 27, Switzerland.
4. Mook, W.G., 2000. Environmental Isotopes in the Hydrological Cycle Principles and Applications. International atomic energy agency and United Nations educational, scientific and cultural organization Vol 1, 2 and 3.
5. Namibia Water Resources Management Review, (2003). Strategic Water Resources Assessment: Theme Report. Ministry of Agriculture, Water, and Rural Development. Windhoek: Author.

Journals

1. Ambach, W., Elsiisser, M., Moser, H., Rauert, W., Stichler W., Trimbom, P., 1975. Variationendes Gehaltesan Deuterium, Sauerstoff-18 und Tritium wahrend einzelner Niederschliige, Warser und Leben, 27,186-192.
2. Andreo, B., Lin A.C., Carrasco, F., Jime´nez de Cisneros C., Caballero F., Mudry J., 2003. Influence of rainfall quantity on the isotopic composition (^{18}O and ^{2}H) of water in mountainous areas. Application for groundwater research in the Yunquera-Nieves karst aquifers (Spain).
3. Bershaw, J., Penny, S. M., and Garzione, C. N. 2012. Stable isotopes of modern water across the Himalaya and eastern Tibetan Plateau: Implications for estimates of paleoelevation and paleoclimate, J. Geophys. Res., 117, D02110, doi:10.1029/2011JD016132.
4. Bittner, A., 2006. Desk Study Report: Cuvelai-etosha Groundwater Investigation. Bittner Water Consult CC. Windhoek, Namibia: BGR internal report.
5. Celle-Jeanton, H., Travy, Y., Blavoux, B., 2001. Isotopic typology of the precipitation in the Western Mediterranean region at three different time scales. Geophys. Res. Lett. 28, 1215–1218.
6. Christelis, G., Struckmeier, W., 2001. Groundwater in Namibia, an Explanation to the Hydrogeological Map. Windhoek. ESRI, 2011. ArcGIS Desktop: Release 10.
7. Clark., Frits., 1997., Environmental isotopes now routely contribute to the stable isotopic composition of water.
8. Cruz Sanjulia´ n, J., Aragua´ s, L., Rozanski, K., Cardenal, J., Hidalgo, M.C., Garcı´a Lopez, S., Martı´nez Garrido, J.C., Moral, F., Olı´as, M., 1992. Sources of precipitation over South-Eastern Spain and groundwater recharge. An isotopic study. Tellus 44B, 226–236.
9. Craig, H., 1961b. Isotopic variation in meteoric waters. Science, 133: 1702-1703.
10. Craig, H., Gordon, I., 1965. Deuterium and oxygen 18 variation in the ocean and marine atmosphere, in Stable Isotopes in Oceanographic Studies and Paleotemperatures,
11. Dansgaard, W., 1964. Stable isotopes in precipitation. - Tellus 16: 436-468.
12. Dragnich, P.A., Dungca, A.C., Pendleton, N.L., Adam, R.T., 2004. The cuvelai-etosha basin management approach, assessing water resource management in the iishana sub-basin. Namibia. P1-22.
13. Du Toit, D., & Sguazzin, T. (1995). Sink or Swim: Water and the Namibian Environment. Swakopmund, NA: Enviroteach.

14. Epstein, S., Mayeda, T., 1953. Variations of 18O contents of water from natural sources. Geochimica et Cosmochimica Acta 4, 213–224.
15. Eriksson, E., 1983. Stable isotopes and tritium in precipitation. In: Guidebook on nuclear techniques in hydrology. Technical Reports Series I.A.E.A. 91, 19–27.
16. Fritz, P., Fontes, J.Ch., 1980. Handbook of Environmental Isotope Geochemistry: The Terrestrial Environment, Vol. 1.Elsevier, Amsterdam
17. Friedman, I., Redfield, A.C., Schoen, B., and Hams J., 1964. Ihe variation of the deuterium content of natural waters in the hydrologic cycle, Rev. Geophysics., 2.1-124.
18. Froehlickh, K., Rozanski, K., Araguas, L.A., 2000. Isotope hydrology: Applied discipline in Earth sciences. P56-61.
19. Gat, J.R., Dansgaard, W., 1972. Stable isotope survey of the fresh water occurrences in Israel and the northem Jordan rift valley, J. Hydrol., 16,177-212.
20. Gat, J.R., Carmi, I., 1970. Evolution of the isotopic composition of atmospheric waters in the Mediterranean Sea area, J. Geophys. Res., 75, 3039–3048, doi:10.1029/JC075i015p03039.
21. Gat, J.R, Airey, P., 2006. Stable water isotopes in the atmosphere/biosphere/lithosphere interface: Scaling-up from the local to continental scale, under humid and dry conditions, Global Planet. Change, 51(1–2), 25–33, doi:10.1016/j.gloplacha.2005.12.004.
22. Gat, J.R., Matsui, E., 1991. Atmospheric water balance in the Amazon basin: an isotopic evapotranspiration model. J. Geophys. Res. 96:13179–88.
23. Gat J.,R, Tzur, Y., 1967. Modification of the isotopic composition of rainwater by processes which occur before groundwater recharge. In Isotopes in Hydrology, pp. 49–60. vienna:Int. At. energy Agency.
24. Hamutoko, J.T., Wanke, H., Koeniger, P., Beyer, M., Gaj, M., 2017. Hydrogeochemical and isotope study of perched aquifers in the Cuvelai-Etosha Basin, Namibia. Isotopes in Environmental and Health Studies P1-16.
25. Hamutoko, J.T., Wanke, H., Voig, h.j., 2016, estimation of groundwater vulnerability to pollution based on drastic in the Niipele sub-basin of the Cuvelai Etosha Basin, Namibia.
26. Honghua Z, Weihong L, Yun W, Zhaoxia, Y., 2016. Characteristics of Stable Isotopes in an Inland Lake and Their Implications for Water Management in Northwestern China. Journal of Water Resource and Protection, 2016, 8, 631-641.
27. Joswiak, D., Yao, T. Wu, G., Xu, B., Zheng, W., 2010. A 70-yr record of oxygen-18 variability in an ice core from the Tanggula Mountains, central Tibetan Plateau, Clim. Past, 6, 219–227, doi:10.5194/cp-6-219- 2010.
28. Kaseke K.F., Wang .L, Wanke H., Turewicz V., Koeniger P., 2016. An Analysis of Precipitation Isotope Distributions across Namibia Using Historical Data. PLoS ONE11(5): e0154598. https://doi.org/10.1371/journal.pone.0154598.
29. Katsuyama, M., Yoshioka, T.,Konohira, E., 2014. Spatial distribution of oxygen-18 and deuterium in stream waters across the Japanese archipelago. Center for the Promotion of Interdisciplinary Education and Research, Kyoto Univ., Kyoto University Higashi Ichijokan, Yoshida Nakaadachi, Sakyo, Kyoto 606-8306, Japan
30. Lai C.T., Ehleringer J.R., 2011. Deuterium excess reveals diurnal sources of water vapor in forest air. Oecologia; 165(1):213–23. doi: 10.1007/s00442-010-1721-2 PMID: 20652594.
31. Mario, Á.C., José, B., Francisco J.P., 2015. Modelling the spatial and seasonal variability of water quality for entire river networks: Relationships with natural and anthropogenic factors. Science of the Total Environment 545–546, P152–162.
32. Masiye N. 2014. The distribution of deuterium and Oxygen-18 isotopes in precipitation in Northern Namibia in relation to other localities in the SADC region. P 1-32.
33. Matsuo, S., Friedman I., 1967. Deuterium content in fractionally collected rain, J. Geophys. Res., 72,63746376.

34. Mendelsohn JM, Jarvis A, Robertson T., 2013. A profile and atlas of the Cuvelai-Etosha basin: raison &
35. Gondwana collection.
36. Mendelsohn, J., Obeid, S.E., Roberts, C., 2000. A profile of North –Central Namibia: Gamsberg Macmillan publisher, Windhoek, Namibia.
37. Mendelsohn, J., Weber. B., 2011. The Cuvelai Basin its water and people in Angola and Namibia. ISBN 978-99916-780-6-1.
38. Merlivat, M., and Jouzel, J., 1979. Global climatic interpretation of the deuterium- oxygen-18 relationship for precipitation, J. Geophys.Res., 84,5029-5033.
39. Miyake, Y., Matsubaya O., Nishihara, C., 1968. An isotopic study on meteoric precipitation, Pap. Meteor. Geophys., 19.243-266.
40. Obiefuna GI, Orazulike DM., 2011. The hydrochemical characteristics and evolution of groundwater in semiarid Yola Area, Northeast, Nigeria. Res J Environ Earth Sci. 2011;3:400–416.
41. Plata, A., 1994. Composicio´n iso´ topica de las precipitaciones y aguas subterra´ neas de la Penı´nsula Ibe´rica. Centro de Estudios y Experimentacio´ n de Obras Pu´ blicas,Vol. 39. Madrid, Spain.
42. Ploethner, D., Sengpiel, K.P., Bittner, A., 1997. Correlation between the Helicopter Geophysical Data and the Hydrogeology along Flight Line Ondangwa - Tsumeb; Ohangwena and Oshikoto.
43. Putthividhya, A., Koonthanakulvong, S., 2011. A case study of stable isotope fingerprinting for surface water and groundwater origin and dynamic interactions in Thailand. Chulalongkorn University, Bangkok, Thailand, Thailand 10330.
44. Ogrinc, N., Kanduc, T., Stichler, W., Vrec, P., 2008. Spatial and seasonal variations in δ18O and δD values in the River Sava in Slovenia. Journal of Hydrology, 359, 303– 312.
45. Rindsberger, M., Magaritz, M., Carmi, I., Gilad, D., 1983. The relation between air mass trajectories and the water isotope composition in the Mediterranean Sea area. Geophys. Rev. Lett. 10, 43–46.
46. Rozanski, K., Aragua´ s, L., Gonfiantini, R., 1992. Relation between long-term trend of oxygen-18 isotope composition of precipitation and climate. Science 258, 982–985.
47. Rozanski, k., Araguas, L.A. Gonftantini, R., 1993. Isotopic Patterns in Modern Global Precipitation. International Atomic Energy Agency, P.O. Box 100,1100-Vienna, Austria.
48. Siegenthaler, V., Oeschger, H., 1980. 18O in precipitation: correlation with temperature and altitude on a regional scale. Nature 285, 314–316.
49. Siegenthaler, U., and Matter, H.,1983 Dependence of SL'O and SD in precipitation on climate, in Paleoclimote and Paleowaters: A Collection of environmental Isotope Studies, pp. 37-51, Intemational Atomic Energy Agency. Vienna, Austria.
50. Stengel, H.W. 1963. Wasserwirtschaft – Waterwese – Water Affairs in S.W.A. Afrika. Verlag Der Kreis, Windhoek, Namibia, 467pp.
51. Stumpp C, Klaus J, Stichler W., 2014. Analysis of long-term stable isotopic composition in German precipitation. Journal of Hydrology. 517:351–61.
52. Taylor, C.B., 1972. The vertical variations of the isotopic concentrations of tropospheric water vapow over continental Europe and their relationship to tropospheric structure, DSIR Repot?lNS-R-107,44pp., Lower Hun, New Zealand.
53. Tian, L., Masson-Delmotte, V., Stievenard, M.,Yao, T., Jouzel, J., 2001, Tibetan Plateau summer monsoon northward extent revealed by measurements of water stable isotopes, J. Geophys. Res., 106(D22), 28,081–28,088, doi:10.1029/2001JD900186.
54. Turewicz V., 2012. Stable isotopes of waters in Namibia [bachelor thesis]. Cologne: University of Cologne.

55. Van Wyk E., Van Tonder G., Vermeulen D., 2011. Characteristics of local groundwater recharge cycles in South African semi-arid hard rock terrains-rainwater input. Water SA. 37(2):147–54.
56. Vuille, M., Werner, M., Bradley, R., and Keimig, F., 2005. Stable isotopes in precipitation in the Asian monsoon region, J. Geophys. Res., 110, D23108, doi:10.1029/2005JD006022.
57. Wanke, H., Nakwafila, A., Hamutoko, J.T., Lohe, C., Neumbo, F., Petrus I., David A., Beukes, H., Masule, N., Quinger, M., 2014. Hand dug wells in Namibia: An underestimated water source or a threat to human health
58. West, A., February, E., Bowen, G., 2011. Creating a map of stable isotopes in tap water across South Africa for hydrological, ecological and forensic applications. Botany Department, University of Cape Town. WRC Report No. KV 284/11ISBN 978-1-4312-0173-0.
59. West, A., February, E., Bowen, G., 2013. Spatial analysis of hydrogen and oxygen stable isotopes ("isoscapes") in ground water and tap water across South Africa
60. Welp, L.R., Lee, X., Griffis., T.J., Wen, X.F., Xiao W., Li S, et al., 2012. A meta-analysis of water vapor deuteriumexcess in the midlatitude atmospheric surface layer. Global Biogeochem Cycles. 26(3):GB3021. doi: 10.1029/2011gb004246.
61. Yurtsever, Y., Araguas L.A., 1993. Environmental isotope applications in hydrology: an overview of the iaea's activities, experiences, and prospects. Isotope Hydrology Section Department of Research & Isotopes, International Atomic Energy Agency (IAEA), Vienna, Austria.
62. Yi, Y., Gibson, J.J., Cooper, L. W., Hélie, J.F., Birks, S.J., McClelland, J.W., Holmes, R.M., Peterson, B.J., 2012. Isotopic signals (18O, 2H, 3H) of six major rivers draining the pan-Arctic watershed. Global biogeochemical cycleS, vol. 26, GB1027, doi:10.1029/2011GB004159.
63. Zhao, L., Wang, L., Liu, X , Xiao, H , Ruan, Y , Zhou, M., 2014. The patterns and implications of diurnal variations in the d-excess of plant water, shallow soil water and air moisture. Hydrology and Earth System Sciences. ; 18(10):4129–51.

Websites

64. ihs@iaea.org www.iaea.org/water
65. https://www.yr.no/place/South_Africa/Northern_Cape/Upington/statistics.html

8. Appedix

Sample ID	latitude	longitude	δ^{18}O (‰)	s.d.	δ^{2}H(‰)	s.d.	D-excess	pH	EC (us/cm)	Turbidity (FAU)
NM-1	-17.98953	16.14	-9.02	0.19	-65.9	0.9	6.3	7.940000	3.620000	532
NM-2	-17.43828	15.08	-4.84	0.16	-34.9	0.8	3.8	8.130000	22.700000	125
NM-3	-17.45436	15.08	-4.78	0.06	-31.0	0.7	7.3	7.770000	35.600000	390
NM-4	-17.48552	15.06	-4.91	0.11	-29.8	0.6	9.4	7.260000	23.200000	46
NM-5	-17.51951	14.98	-6.01	0.16	-36.2	0.8	11.9	7.260000	20.700000	66
NM-6	-17.49432	14.96	-5.60	0.09	-32.8	0.6	12.0	7.960000	17.850000	72
NM-7	-17.49723	14.89	-3.53	0.17	-21.0	0.7	7.3	8.130000	22.800000	209
NM-8	-17.294	14.58	-1.84	0.11	-13.7	0.6	1.1	6.700000	109.000000	165
NM-9	-16.872636	14.81	-3.22	0.04	-18.7	1.3	7.1	6.990000	128.400000	185
NM-10	-16.828907	14.89	-3.33	0.15	-20.2	0.7	6.4	7.110000	78.100000	209
NM-11	-16.959312	15.59	-5.39	0.10	-31.1	0.9	12.0	7.560000	20.010000	48
NM-12	-16.909623	15.52	-5.72	0.11	-34.3	0.3	11.4	7.900000	25.500000	53
NM-13	-16.842195	15.46	-6.02	0.13	-38.1	0.9	10.1	7.540000	20.210000	32
NM-14	-16.622491	15.05	-3.18	0.04	-18.3	0.7	7.1	6.640000	98.900000	261
NM-15	-16.614341	15.06	-3.69	0.04	-23.5	0.8	6.0	6.880000	78.600000	239
NM-16	-16.592511	15.07	-3.35	0.11	-18.8	1.5	7.9	6.830000	102.050000	55
NM-17	-16.573395	15.09	-4.15	0.06	-26.6	0.6	6.6	7.240000	72.500000	88
NM-18	-16.534201	15.13	-2.62	0.11	-24.9	0.9	-4.0	7.440000	68.800000	115
NM-19	-16.488761	15.20	-4.61	0.12	-26.2	0.7	10.8	7.200000	133.500000	76
NM-20	-16.357342	15.29	-5.79	0.11	-37.3	0.5	9.0	7.630000	47.000000	56
NM-21	-16.410946	15.26	-5.03	0.11	-29.4	0.4	10.8	8.170000	34.000000	55
NM-22	-17.039845	14.74	-5.01	0.17	-28.4	0.7	11.6	8.210000	39.400000	171
NM-23	-17.428399	14.61	-5.98	0.08	-40.2	0.7	7.7	8.140000	36.800000	83
NM-24	-17.432	14.62	-3.40	0.19	-22.7	0.6	4.5	8.870000	41.800000	31
NM-25	-17.459617	15.12	-3.68	0.05	-25.5	0.8	4.0	7.960000	45.600000	499

NM-26	-17.455093	15.17	-1.73	0.08	-14.6	0.8	-0.8	8.880000	40.900000	248
NM-27	-17.45469	15.19	-0.80	0.10	-8.0	0.3	-1.5	8.310000	481.000000	1110
NM-28	-17.447919	15.22	-1.49	0.11	-13.3	0.2	-1.4	8.710000	135.900000	319
NM-29	-17.448732	15.26	-3.40	0.15	-21.4	0.4	5.8	9.090000	31.900000	187
NM-30	-17.441022	15.31	-2.24	0.13	-17.8	0.9	0.1	8.910000	53.400000	491
NM-31	-17.445071	15.35	-3.27	0.17	-21.3	0.7	4.9	8.870000	63.000000	161
NM-32	-17.456195	15.39	-2.33	0.10	-15.9	0.7	2.7	8.110000	64.900000	261
NM-33	-17.459832	15.42	-0.78	0.23	-7.5	1.0	-1.3	8.510000	217.000000	425
NM-34	-17.428057	15.46	-3.00	0.17	-12.4	0.8	11.6	8.870000	102.000000	0
NM-35	-17.462199	15.44	-1.82	0.09	-11.5	1.1	3.1	8.640000	283.000000	113
NM-36	-17.46514	15.46	-1.74	0.09	-12.6	0.9	1.4	7.870000	66.900000	323
NM-37	-17.47164	15.51	-1.27	0.09	-11.6	0.4	-1.4	8.860000	80.700000	584
NM-38	-17.473434	15.57	-2.56	0.20	-15.7	1.0	4.8	8.880000	117.400000	293
NM-39	-17.468287	15.59	-3.11	0.08	-19.8	0.9	5.0	8.500000	44.800000	72
NM-40	-17.458866	15.62	-3.10	0.28	-14.9	0.5	9.9	9.040000	109.200000	520
NM-41	-17.448552	15.65	-3.37	0.07	-19.2	0.4	7.8	8.560000	77.600000	219
NM-42	-17.445821	15.66	-3.22	0.11	-17.9	0.3	7.8	8.890000	103.100000	480
NM-43	-17.447157	15.70	-3.63	0.08	-19.5	0.9	9.6	8.730000	53.700000	205
NM-44	-17.447513	15.74	-2.31	0.06	-18.2	0.7	0.3	9.020000	84.500000	119
NM-45	-17.447688	15.76	-3.73	0.07	-28.2	0.4	1.6	8.320000	36.600000	116
NM-46	-17.447566	15.79	-4.61	0.15	-30.6	0.8	6.3	8.270000	88.400000	121
NM-47	-17.447069	15.80	-6.74	0.16	-49.3	0.9	4.6	8.060000	102.100000	113
NM-48	-17.449248	15.87	-4.06	0.11	-27.2	1.4	5.3	8.610000	82.400000	105
NM-49	-17.766577	15.69	-4.09	0.20	-27.2	0.3	5.5	8.360000	103.500000	801
NM-50	-17.711439	15.56	-3.39	0.14	-20.1	0.4	7.0	7.770000	95.100000	519
NM-51	-17.649513	15.48	-4.12	0.21	-24.3	1.0	8.6	8.530000	44.900000	234
NM-52	-17.568141	15.11	-0.39	0.17	-4.8	0.8	-1.6	8.200000	99.900000	1110
NM-53	-17.593938	15.18	2.26	0.13	7.1	0.7	-10.9	7.990000	225.000000	1110
NM-54	-17.63915	15.27	-5.08	0.21	-29.2	0.1	11.4	8.280000	78.200000	128
NM-55	-17.663764	15.34	-5.72	0.12	-38.9	0.7	6.8	7.600000	72.400000	88

NM-56	-17.660562	15.39	-2.74	0.19	-15.7	0.4	6.2	8.450000	75.500000	328
NM-57	-17.780508	15.70	-5.17	0.01	-31.5	0.2	9.9	7.350000	88.800000	228
NM-58	-17.786769	15.73	-4.23	0.12	-28.5	0.7	5.3	8.490000	54.300000	231
Arithmetic mean			**-3.65**	**0.12**	**-23.64**	**0.70**	**5.56**	**8.09**	**82.49**	**262.47**

Table 1. Campaign 1 (February) raw and processed data

Sample ID	**latitude**	**longitude**	**$\delta^{18}O$**	**s.d.**	**$\delta^{2}H$**	**s.d.**	**D-excess**	**pH**	**EC (us/cm)**	**Turbidity (FAU)**
NM-70	14.893983	-17.497187	-11.84	0.10	-86.3	1.0	8.4	6.960000	17.220000	142
NM-71	14.893983	-17.497187	-10.47	0.11	-76.3	1.7	7.5	7.620000	15.960000	69
NM-72	14.839311	-17.473831	-10.52	0.19	-76.7	1.9	7.4	6.960000	59.100000	77
NM-73	14.647376	-17.429287	-11.70	0.09	-84.7	0.5	8.9	6.840000	18.220000	84
NM-74	14.651518	-17.422263	-13.51	0.11	-96.6	1.2	11.6	6.850000	16.440000	104
NM-75	14.643619	-17.430374	-12.46	0.25	-92.0	1.2	7.6	7.560000	16.540000	80
NM-76	14.607302	-17.428073	-11.28	0.12	-84.4	1.2	5.9	7.300000	29.200000	98
NM-77	15.117361	-17.459877	-10.98	0.20	-81.4	1.2	6.5	8.200000	22.200000	197
NM-78	15.173382	-17.455826	-10.57	0.14	-79.6	0.7	5.0	7.190000	745.000000	110
NM-79	15.195418	-17.454398	-9.58	0.05	-71.7	0.8	4.9	7.020000	117.100000	126
NM-80	15.219847	-17.448050	-5.78	0.16	-41.5	1.2	4.8	7.120000	39.300000	40
NM-81	15.264620	-17.448680	-6.26	0.07	-43.2	0.6	6.9	7.160000	36.100000	53
NM-82	15.307682	-17.441116	-12.91	0.23	-93.3	1.6	10.0	7.190000	18.650000	108
NM-83	15.393565	-17.456274	-13.35	0.07	-96.5	0.6	10.3	7.070000	14.400000	98
NM-84	15.419947	-17.460003	-11.19	0.06	-82.0	0.4	7.5	8.130000	26.800000	0
NM-85	15.419929	-17.459994	-13.30	0.11	-98.1	0.4	8.3	7.010000	15.440000	85
NM-86	15.457623	-17.465296	-12.34	0.07	-90.4	0.9	8.3	8.290000	22.300000	97
NM-87	15.512384	-17.471833	-11.71	0.21	-87.5	1.5	6.2	8.300000	44.200000	233
NM-88	15.568397	-17.473643	-11.78	0.19	-88.3	0.7	5.9	7.200000	36.700000	125

NM-89	15.593265	-17.468430	-11.14	0.17	-84.3	1.1	4.8	8.160000	49.200000	220
NM-90	15.622307	-17.458908	-10.44	0.14	-79.9	1.0	3.6	7.080000	46.100000	187
NM-91	15.699765	-17.447276	-10.73	0.04	-81.1	0.6	4.7	7.050000	33.000000	152
NM-92	15.749980	-17.447684	-11.36	0.11	-83.3	0.6	7.6	7.460000	32.100000	187
NM-93	15.762547	-17.447821	-10.68	0.09	-78.4	0.8	7.1	6.920000	38.500000	65
NM-94	15.791574	-17.447603	-10.53	0.27	-75.8	1.3	8.4	7.660000	50.800000	219
NM-95	15.873318	-17.449229	-11.03	0.06	-81.3	0.5	6.9	7.890000	43.900000	174
NM-96	15.111736	-17.568189	-11.25	0.13	-83.5	0.7	6.5	7.920000	25.000000	126
NM-97	15.176452	-17.594142	-11.55	0.15	-86.9	1.1	5.6	7.920000	23.300000	102
NM-98	15.273731	-17.639172	-12.19	0.20	-91.9	1.2	5.6	6.840000	32.900000	107
NM-99	15.342697	-17.664046	-12.29	0.07	-93.9	0.2	4.4	7.180000	34.800000	0
NM-100	15.377805	-17.667676	-10.39	0.09	-76.7	0.9	6.5	6.590000	19.990000	64
NM-101	14.884677	-16.847033	-8.24	0.01	-61.0	0.2	4.9	7.400000	21.480000	100
NM-102	14.879576	-16.859480	-7.30	0.11	-53.9	0.6	4.5	7.520000	37.200000	45
NM-103	14.893143	-16.836726	-10.01	0.13	-69.9	0.7	10.2	6.770000	19.540000	213
NM-104	15.182409	-16.495079	-5.13	0.06	-30.0	1.0	11.0	6.680000	31.400000	61
NM-105	15.592364	-16.959312	-11.76	0.14	-86.0	0.7	8.1	7.730000	16.730000	14
NM-106	14.959922	-17.494328	-13.40	0.14	-100.1	1.5	7.1	7.890000	13.040000	57
NM-107	14.893976	-17.497194	-11.56	0.23	-85.1	1.7	7.4	7.700000	39.200000	210
NM-108	14.893556	-16.825917	-8.63	0.17	-62.5	1.0	6.5	0.000000	0.000000	0
NM-109	14.889951	-16.853241	-8.51	0.12	-61.3	1.0	6.8	7.490000	34.600000	257
NM-110	15.388920	-17.660776	-9.80	0.04	-73.4	0.4	5.0	6.780000	33.700000	165
NM-111	15.476575	-17.649481	-11.44	0.10	-82.8	1.2	8.8	7.350000	26.500000	177
NM-112	15.555007	-17.711673	-11.43	0.09	-81.5	0.4	9.9	7.150000	38.800000	66
NM-113	15.637759	-17.761231	-11.67	0.15	-85.0	0.8	8.3	7.480000	71.900000	117
NM-114	15.684991	-17.766810	-11.27	0.14	-82.0	0.9	8.1	7.560000	56.700000	193
NM-115	15.698773	-17.781977	-12.49	0.08	-90.1	1.0	9.8	7.830000	35.500000	144
NM-116	15.727951	-17.787691	-11.42	0.11	-83.0	0.7	8.3	7.890000	51.300000	210
NM-117	15.727939	-17.787685	-10.07	0.14	-73.4	0.5	7.1	7.860000	83.500000	572
NM-118	15.727936	-17.787685	-11.71	0.16	-84.8	1.2	8.8	7.600000	54.600000	326

NM-119	15.727933	-17.787685	-10.52	0.10	-77.9	0.7	6.3	7.010000	52.500000	230
NM-120	15.727930	-17.787687	-11.62	0.10	-87.2	0.9	5.8	7.370000	31.100000	235
NM-121	14.906425	-17.767326	-11.85	0.06	-87.1	0.6	7.7	6.990000	36.300000	81
NM-122	15.136263	-17.889948	-12.16	0.13	-89.5	0.3	7.7	7.080000	38.100000	77
NM-123	15.431856	-17.787101	-10.32	0.14	-77.2	0.8	5.4	7.050000	72.400000	244
NM-124	15.136263	-17.889948	-10.06	0.11	-75.6	0.5	4.8	7.630000	85.600000	466
NM-125	15.185219	-17.875203	-9.38	0.17	-69.9	0.7	5.2	7.280000	45.000000	165
NM-126	15.347732	-17.789733	-11.90	0.13	-87.2	0.2	8.0	6.680000	34.100000	118
Arithmetic mean			**-10.86**	**0.12**	**-79.74**	**0.87**	**7.11**	**7.24**	**49.14**	**141.61**

Table 2. Campaign 2 (March) raw and processed data

Sample ID	**Longitude**	**Latitude**	**$\delta^{18}O$**	**s.d.**	**$\delta^{2}H$**	**s.d.**	**D-excess**	**pH**	**EC (uS/cm)**	**Turbidity (FAU)**
202	15.78847	-17.4477	-7.46	0.05	-60.1	0.2	-0.4	5.3	44.3	80
204	15.59304	-17.4685	-3.66	0.11	-41.9	0.6	-12.6	6	58	78
205	14.65142	-17.4224	-5.34	0.08	-51.4	0.8	-8.6	6.58	126.8	48
206	15.63944	-17.763	-2.93	0.14	-31.9	0.6	-8.5	6.26	87.5	>1110
207	15.39359	-17.4562	-4.30	0.26	-40.2	0.7	-5.8	5.79	44.3	182
208	15.32169	-17.4374	-6.16	0.12	-55.7	0.5	-6.4	6.02	67.1	250
211	15.27518	-17.6388	-4.08	0.10	-44.4	0.3	-11.7	6.61	47.3	289
216	15.33807	-17.6647	-5.39	0.19	-48.9	1.2	-5.8	6.63	49.8	226
217	15.81401	-17.8268	-3.54	0.10	-37.0	0.2	-8.7	5.31	46.4	117
219	14.9597	-17.4943	-7.70	0.14	-63.0	0.6	-1.4	6.75	31.6	130
220	17.96328	-18.7781	-4.89	0.14	-50.2	0.4	-11.1	5.97	232	32
221	15.79862	-17.8194	-2.55	0.09	-30.6	0.5	-10.3	5.26	44.4	88
222	15.07654	-17.4379	-7.82	0.13	-62.7	0.3	-0.1	6.6	149.8	>1110
223	15.93123	-17.5178	3.49	0.30	-0.5	0.4	-28.4	5.34	42	45

225	15.94233	-18.5007	-8.14	0.22	-67.5	0.7	-2.4	6.9	135.9	411
226	15.11713	-17.4599	-6.46	0.01	-54.2	0.4	-2.5	6.08	32.5	153
227	15.7717	-17.4478	-5.85	0.12	-55.8	0.3	-9.1	5.78	32.1	77
229	15.80263	-17.8234	-6.19	0.17	-54.1	0.8	-4.6	5.52	48	64
230	15.058	-17.488	-7.52	0.10	-61.3	0.2	-1.2	5.46	35.1	234
235	15.08443	-17.5619	-5.92	0.02	-56.3	0.3	-9.0	6.18	26.1	155
237	15.17725	-17.5943	-5.34	0.08	-51.4	0.8	-8.6	6.57	53.5	256
239	15.04351	-17.4938	-2.93	0.14	-31.9	0.6	-8.5	5.77	22.3	340
240	15.69955	-17.4472	-4.08	0.10	-44.4	0.3	-11.7	6	96	298
241	15.51187	-17.4719	3.62	0.06	-0.4	0.3	-29.4	6.08	62.5	329
242	15.90992	-17.4139	-6.10	0.10	-54.7	0.9	-5.9	5.3	51.4	61
243	14.93705	-17.5678	-5.02	0.07	-43.6	0.5	-3.5	6.49	43.7	143
245	14.98147	-17.5197	-5.08	0.10	-46.5	0.5	-5.8	5.81	29.8	73
247	15.30763	-17.4411	-2.96	0.06	-33.1	0.3	-9.4	6.08	74.1	>1110
249	15.82451	-17.7186	-4.53	0.10	-46.7	0.6	-10.4	6.07	45.2	76
250	15.19432	-17.4548	-7.99	0.11	-65.2	0.5	-1.3	6.09	142.7	>1110
251	15.47659	-17.6495	-3.84	0.05	-42.4	0.3	-11.6	6.63	65.7	375
252	15.87195	-17.4497	-5.96	0.11	-53.5	0.4	-5.8	5.14	45.2	56
256	15.55501	-17.7115	-3.13	0.10	-37.9	0.3	-12.9	7	115.3	629
303	14.83995	-17.4739	-7.53	0.06	-62.2	0.4	-2.0	6.65	82.4	231
325	15.07821	-17.4544	-7.10	0.09	-58.7	0.5	-1.9	6.36	62.4	498
252			-7.01	0.07	-60.9	0.5	-4.8			
255			-5.14	0.10	-52.7	0.3	-11.5			
256			-1.93	0.11	-26.7	0.2	-11.2			
301			-2.32	0.06	-30.5	0.3	-11.9			
307			-7.60	0.17	-64.2	0.2	-3.4			
251			-4.41	0.15	-42.9	0.4	-7.6			
Arithmetic mean			**-4.85**	**0.11**	**-46.78**	**0.48**	**-7.99**	**6.07**	**67.81**	**194.32**

Table 1. Campaign 3 (April) raw and processed data

Sample ID	Longitude	Latitude	$\delta^{18}O$	s.d.	$\delta^{2}H$	s.d.	D-excess	Ph	EC (µs/cm)	Turbidity (FAU)
NT-01	17.99884	-18.31633	-3.39	0.19	-15.91	0.40	11.21	5.96	110.5	602
NT-02	18.16628	-17.95174	1.19	0.10	-4.82	0.87	-14.31	7.09	226	770
NT-03	18.23309	-17.67524	-5.55	0.15	-51.30	0.46	-6.93	6.95	91.2	49
NT-04	17.12712	-17.41149	3.20	0.04	0.54	0.39	-25.03	8.15	94.7	>1110
NT-05	17.21206	-17.45966	2.08	0.18	-5.07	0.44	-21.74	7.43	80	0.11
NT-06	16.77538	-17.7138	2.65	0.13	17.19	0.57	-4.05	8.46	79.7	479
NT-07	16.79469	-17.68347	6.19	0.17	21.97	1.20	-27.57	8.6	86	702
NT-08	16.81604	-17.6484	3.37	0.12	10.64	0.41	-16.30	7.44	82.5	44
NT-09	16.80619	-17.62851	1.84	0.06	-0.17	0.39	-14.89	7.85	389	150
NT-10	16.81554	-17.64416	-2.17	0.11	-21.56	0.46	-4.22	7.48	135.9	73
NT-11	17.09595	-17.57787	3.98	0.11	17.56	0.37	-14.31	7.52	243	>1110
NT-12	17.38876	-17.57974	6.41	0.08	24.79	0.57	-26.50	7.57	265	>1110
NT-13	17.40005	-17.69548	3.21	0.10	16.70	0.83	-8.95	8.07	155.2	>1110
NT-14	16.86228	-17.58113	3.46	0.10	15.97	0.38	-11.73	8.11	354	>1110
NT-15	16.65795	-17.54439	3.36	0.11	13.96	0.41	-12.94	8.49	145	350
NT-16	16.49718	-17.47816	5.56	0.21	22.41	1.41	-22.09	8.43	519	>1110
NT-17	16.4558	-17.47535	0.91	0.05	-3.62	0.52	-10.90	8.52	292	>1110
NT-18	16.22135	-17.49624	-2.31	0.15	-28.91	0.31	-10.46	8.52	162.3	190
NT-19	16.11914	-17.50773	-2.92	0.12	-28.71	0.58	-5.37	8.48	134.7	259
NT-20	15.91026	-17.51952	-4.74	0.12	-45.34	0.87	-7.45	8.14	104.6	160
NT-21	15.87949	-17.45007	-6.13	0.14	-58.1	0.9	-9.04	8.03	66.2	50
NT-22	15.8102	-17.44559	3.31	0.10	-3.9	0.6	-30.43	7.67	55.6	213
NT-23	15.69446	-17.45253	2.85	0.12	-2.8	0.7	-25.64	7.64	221	614

NT-24	15.56616	-17.47462	7.65	0.23	29.6	1.0	-31.60	8.29	356	>1110
NT-25	15.41856	-17.462663	10.29	0.07	43.5	0.3	-38.81	7.75	776	>1110
NT-26	15.29396	-17.44078	2.03	0.13	-3.8	0.6	-20.08	8.3	85.5	262
NT-27	15.19271	-17.45499	-0.45	0.28	-19.7	1.1	-16.09	8.19	300	>1110
NT-28	15.14945	-17.44174	1.45	0.08	-15.0	0.6	-26.60	7.63	44.9	116
NT-29	15.02712	-17.50789	12.44	0.19	50.9	1.3	-48.58	7.36	367	>1110
NT-30	14.9667	-17.5286	1.44	0.18	-12.1	1.0	-23.64	7.64	117.9	164
NT-31	14.92336	-17.61123	-2.17	0.06	-33.5	0.4	-16.21	8.06	38.5	108
NT-32	14.90772	-17.71297	2.34	0.10	6.1	1.0	-12.61	7.98	135.3	>1110
NT-33	14.92687	-17.79128	1.38	0.18	-5.9	1.1	-16.86	8.1	96.7	308
NT-34	14.99633	-17.81902	3.06	0.17	0.9	0.9	-23.59	8.04	195.2	>1110
NT-35	15.03678	-17.88745	3.36	0.03	0.3	0.5	-26.60	9.27	260	141
NT-36	14.43957	-17.86441	-1.89	0.21	-31.5	1.2	-16.32	8.35	52.2	187
NT-37	14.87212	-17.85649	2.37	0.08	-4.9	0.5	-23.83	8.35	223	83
NT-38	15.34802	-17.78775	7.95	0.18	29.4	1.3	-34.19	8.29	127.2	510
NT-39	15.22052	-17.84297	7.83	0.04	27.0	0.8	-35.60	7.98	206.5	>1110
NT-40	15.29062	-17.82005	1.83	0.17	-1.0	0.6	-15.61	8.19	357	>1110
NT-41	15.34802	-17.78775	2.58	0.23	-1.1	0.8	-21.71	8.29	127.2	510
NT-42	15.46758	-17.78802	-1.96	0.19	-27.7	0.9	-12.00	8.32	145.2	330
NT-43	15.53973	-17.88445	3.98	0.21	1.0	0.5	-30.82	8.13	457	>1110
NT-44	15.43665	-17.95172	5.81	0.21	8.9	0.8	-37.61	7.37	210.9	36
NT-45	15.60639	-17.79277	0.12	0.13	-17.2	0.7	-18.16	8.21	55.1	81
NT-46	15.66709	-17.76382	9.55	0.25	33.5	1.5	-42.91	7.89	321	>1110
NT-47	15.53498	-17.71066	6.69	0.18	19.4	0.3	-34.13	8.08	270	>1110
NT-48	15.45702	-17.66093	-0.46	0.20	-22.4	0.4	-18.67	8.17	78.1	226
NT-49	15.35785	-17.67065	6.70	0.10	20.1	0.7	-33.55	8.14	157.7	>1110
NT-50	15.27201	-17.63931	2.63	0.07	-4.5	0.7	-25.57	8.15	86.2	483
NT-51	15.14417	-17.57942	-3.40	0.18	-39.7	1.3	-12.50	8.14	76.6	161
NT-52	15.09624	-17.4647	5.51	0.22	8.5	0.6	-35.59	7.23	102.4	>1110
NT-53	14.79359	-17.45292	6.18	0.08	8.8	0.4	-40.60	7.43	92.7	472

NT-54	14.5331	-17.41928	0.06	0.19	-16.8	0.5	-17.29	7.36	156	70
NT-55	15.34431	-17.47173	0.62	0.27	-15.3	1.1	-20.19	7.36	202.4	168
NT-56	15.39084	-17.5737	6.45	0.08	23.7	0.9	-27.88	7.8	578	>1110
NT-57	15.4536	-17.64985	3.23	0.05	-4.7	0.4	-30.55	7.63	45.1	43
NT-58	15.47584	-17.68935	5.00	0.10	12.5	0.5	-27.50	7.92	457	>1110
NT-59	15.48831	-17.74782	5.06	0.10	10.5	0.3	-29.96	8.02	171.3	>1110
NT-60	15.58449	17.82603	1.52	0.21	-7.5	1.2	-19.67	8.2	173.6	285
Nt-61	15.78081	-17.79852	3.37	0.12	-1.8	0.7	-28.77	7.47	68	242
Nt-62	15.92417	-17.86586	1.96	0.12	-12.0	0.6	-27.66	7.49	73.8	211
Nt-63	16.09206	-17.96728	3.47	0.27	-2.8	0.9	-30.53	7.42	166.8	48
Nt-64	16.27246	-18.09969	-1.29	0.18	-14.5	0.9	-4.19	7.61	162.4	>1110
Nt-65	16.45025	-18.24831	3.57	0.10	11.2	0.5	-17.35	7.19	121.4	>1110
Nt-66	16.79115	-18.4478	5.06	0.21	14.6	1.2	-25.91	7.94	156	186
Arithmetic mean			**2.57**	**0.14**	**-0.96**	**0.72**	**-21.48**	**7.90**	**190.06**	**247.22**

Table 1. Campaign 4 (May) raw and processed data.

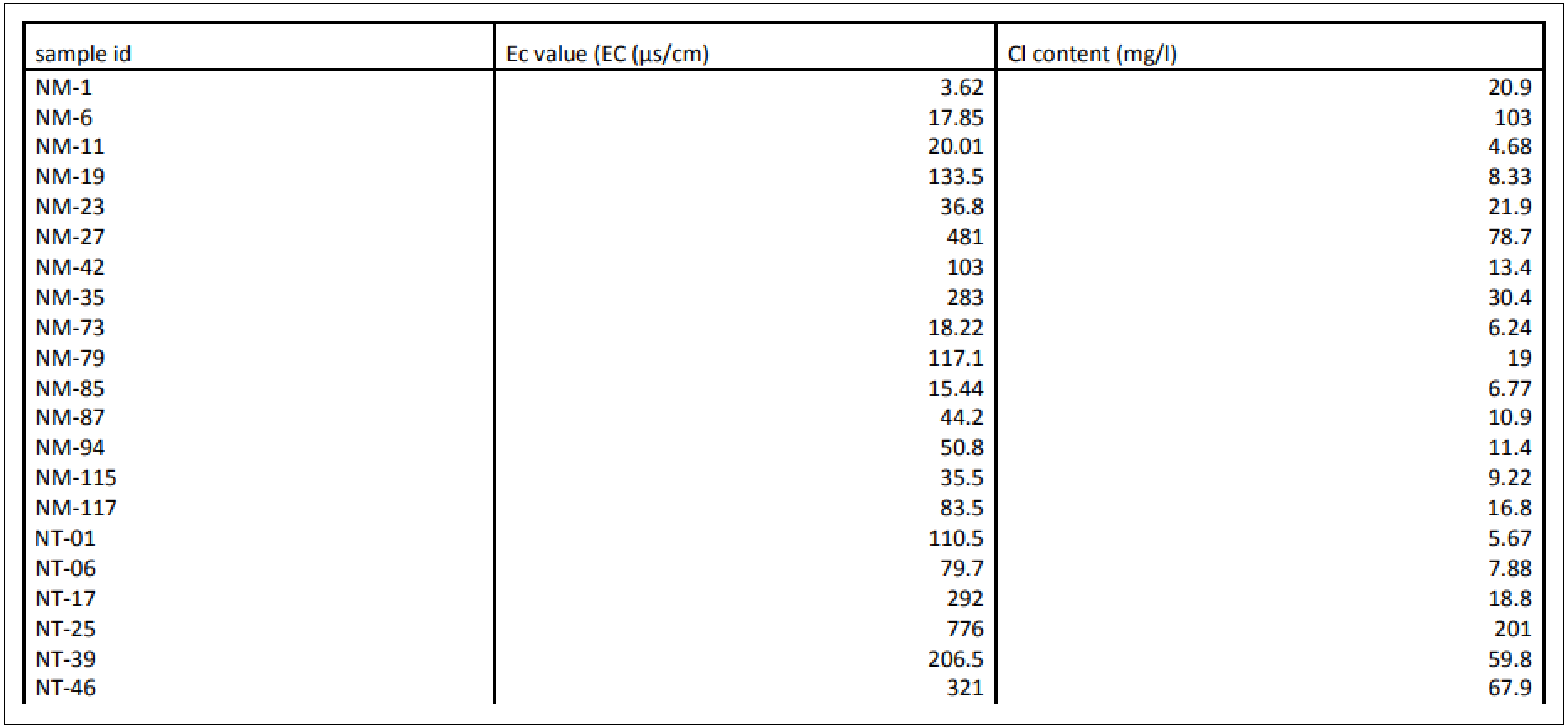

sample id	Ec value (EC (µs/cm)	Cl content (mg/l)
NM-1	3.62	20.9
NM-6	17.85	103
NM-11	20.01	4.68
NM-19	133.5	8.33
NM-23	36.8	21.9
NM-27	481	78.7
NM-42	103	13.4
NM-35	283	30.4
NM-73	18.22	6.24
NM-79	117.1	19
NM-85	15.44	6.77
NM-87	44.2	10.9
NM-94	50.8	11.4
NM-115	35.5	9.22
NM-117	83.5	16.8
NT-01	110.5	5.67
NT-06	79.7	7.88
NT-17	292	18.8
NT-25	776	201
NT-39	206.5	59.8
NT-46	321	67.9

Table 5. Electrical conductivity and chloride result data.